Identifying Disconnected Agents in Multiagent Systems via External Estimators

Rongrong Qian, *Member, IEEE*, Zhisheng Duan, *Senior Member, IEEE*, Yuan Qi, Tao Peng, *Member, IEEE*, and Wenbo Wang, *Senior Member, IEEE*

***Abstract*—This article addresses the problem of identifying disconnected agents in multiagent systems via external estimators. Specifically, we employ external estimators with an appropriately designed decision rule to identify the disconnectedness (i.e., the status of being disconnected) between two arbitrarily chosen agents in formation-control multiagent systems. The design of the decision rule is inspired by the unit-root testing problem of autoregressive time series. To make the best possible decision, a best-effort procedure is also proposed. Then, by introducing the concept of *connected components* (or just *components*) in graph theory, and using the methods of consensus analysis and time-series analysis, we develop an analytical framework to show the theoretical performance of the designed decision rule. A particularly important result shown by our analysis is that the miss probability of the decision rule can converge to 0 as the number of data samples increases. Finally, simulation results validate the performance of the decision rule and the best-effort procedure, showing that they can perform well even in small samples.**

***Index Terms*—Connectivity, consensus analysis, estimation, multiagent systems, time-series analysis.**

I. Introduction

RECENTLY, the use of multiagent systems, such as multiunmanned aerial vehicle (multi-UAV) systems and multirobot systems, has emerged as a promising solution for accomplishing a variety of civilian and military missions [1]–[29], [45]. Autonomous agents can interact with each other via a communication network to achieve certain global objectives [1], [3], [5]–[7], [10]–[20], [45]. This network is often modeled by a communication graph which is said to be connected if there is a path between every pair of vertices in the graph [18]. With the aim of fully leveraging the benefits of multiagent systems, it is necessary to overcome many unprecedented issues arising from nonideal communication conditions [13], [17], [45]. A differentiating factor in typical multiagent networks compared with the current majority of communication networks is the several-fold increase in the mobility of network nodes [28], [29]. The high mobility of agents can cause multiagent networks to be easily disconnected, that is, some agents are disconnected from others [28], [29].

Manuscript received 13 March 2022; accepted 26 May 2022. Date of publication 24 June 2022; date of current version 17 January 2024. This work was supported in part by the National Natural Science Foundation of China under Grant 61971058, Grant 61801048, Grant T2121002, Grant 61631004, and Grant 62071063; and in part by the Beijing Natural Science Foundation under Grant L202014 and Grant L192002. This article was recommended by Associate Editor S. Nahavandi. *(Corresponding author: Rongrong Qian.)*

Rongrong Qian is with the School of Artificial Intelligence, Beijing University of Posts and Telecommunications, Beijing 100876, China (e-mail: rongrongqian@bupt.edu.cn).

Zhisheng Duan is with the State Key Laboratory for Turbulence and Complex Systems, College of Engineering, Peking University, Beijing 100871, China (e-mail: duanzs@pku.edu.cn).

Yuan Qi is with the School of Electronic Engineering, Beijing University of Posts and Telecommunications, Beijing 100876, China (e-mail: qiyuan@bupt.edu.cn).

Tao Peng and Wenbo Wang are with the Wireless Signal Processing and Network Lab (Key Laboratory of Universal Wireless Communication, Ministry of Education), Beijing University of Posts and Telecommunications, Beijing 100876, China (e-mail: pengtao@bupt.edu.cn; wbwang@bupt.edu.cn).

Color versions of one or more figures in this article are available at https://doi.org/10.1109/TCYB.2022.3180507.

Digital Object Identifier 10.1109/TCYB.2022.3180507

A. State of the Art and Prior Works

There has been significant research related to the estimation, maintenance (preservation), and control of the network connectivity for multiagent systems [1]–[23]. Zhang *et al.* [1] recently proposed a decentralized method to estimate the algebraic connectivity of undirected graphs. Sabattini *et al.* [10] developed a decentralized estimation and control strategy to maintain the strong connectivity of directed communication graphs. Franceschelli *et al.* [14] presented a decentralized algorithm to estimate the eigenvalues of the Laplacian matrix that encodes the network topology of a multiagent system. Yang *et al.* [20] proposed estimating and controlling the global connectivity of a network using only decentralized computations and local communication via a power iteration algorithm. Dimarogonas and Kyriakopoulos [21] provided a distributed control strategy to preserve connectivity by using repulsive and attractive potential fields. De Gennaro and Jadbabaie [23] developed a decentralized algorithm for the connectivity control of a multiagent system. Zavlanos *et al.* [18] provided a theoretical framework for controlling network connectivity and discussed various distributed methods to maintain, control, and increase network connectivity.

Most literature on the network connectivity of multiagent systems employed the assumption that the communication graph is a connected graph [1]–[23]. Nevertheless, in realistic situations, it is impossible for a multiagent system to keep its communication network connected all the time during the system evolution, that is, all-time connectivity may not be ensured [25]. This has motivated further investigations on intermittent connectivity scenarios for multiagent networks [24]–[26]. Kantaros and Zavlanos [24] designed a distributed controller for the agents so that the network connectivity is guaranteed over time, infinitely often. Khodayi-Mehr *et al.* [25] developed a distributed controller that designs sequences of communication events for the agents so that the network can be intermittently connected infinitely often. Aragues *et al.* [26] proposed an intermittent connectivity strategy that allows multiple agents to move on the 1-D cycle graph of the environment.

Very few studies have paid attention to disconnected network scenarios in which neither all-time connectivity nor intermittent connectivity is guaranteed. Being disconnected is the worst-case status of a multiagent network [28], [29], and it would be better to prevent it from happening [1]–[23], but there is no absolute guarantee that a practical multiagent network will never be disconnected. Multiagent systems need the ability to immediately reconnect after their communication networks are disconnected [28], [29], for which identifying the disconnected agents within the systems is a prerequisite. The difficulty in achieving this identification is caused by a lack of available modeling, analysis, and design methods.

B. Contributions

In this article, we consider multiagent systems whose communication networks are disconnected, meaning that all-time and intermittent connectivity cannot be guaranteed. We develop an approach to monitoring the connection status of two arbitrarily chosen agents via external estimators and to identify those that are disconnected, on the basis of the data samples. We show that an appropriately designed decision rule allows external estimators to accomplish this identification. In particular, we prove that the miss probability of the designed decision rule converges to 0 as the number of data samples increases. An interesting finding in the simulations shows that even with a small sample number, both miss and false alarm probabilities can be reduced to below 0.05 in many cases.

The main contributions and novelty of this article can be summarized as follows.

1) Prior works on the network connectivity of multiagent systems have mainly adopted the all-time or intermittent connectivity assumption [1]–[27]. To the best of our knowledge, this article is one of the first to systematically study the disconnected network scenario (Assumption 1), with the aim of identifying disconnected agents.
2) We build a model of external estimators that monitor the connection status of two arbitrarily chosen agents, and design a decision rule to judge whether these two agents are disconnected (Decision Rule 2). The design of the decision rule is inspired by the unit-root testing problem of autoregressive time series, in which the use of an ordinary least squares (OLS)-type estimate is a key ingredient. Moreover, we propose a best-effort procedure to make the best possible decision (Procedure 1).
3) We develop an analytical framework to show the theoretical performance of the designed decision rule. To be specific, the concept of components in graph theory is first introduced to characterize disconnected communication graphs (Definition 1). Based on this concept, the basic equivalence conditions for two agents to be disconnected and connected are derived (Lemma 1). The methods of consensus analysis [31], [32] are then used to build a bridge between the dynamics model of multiagent systems and autoregressive time series (Lemma 5). Finally, the application of time-series analysis [40] reveals the theoretical performance of the decision rule (Theorems 1 and 2).

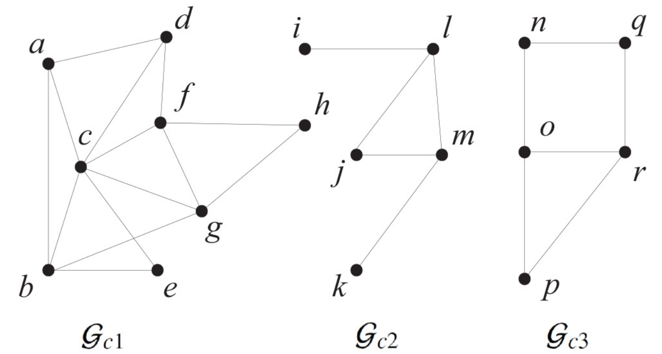

Fig. 1. Disconnected graph $\mathcal{G}$ that has three components, that is, $\mathcal{G}_{c1}$, $\mathcal{G}_{c2}$, and $\mathcal{G}_{c3}$, such that $\mathcal{G} = \mathcal{G}_{c1} \cup \mathcal{G}_{c2} \cup \mathcal{G}_{c3}$. The vertex sets of these components are $V_{\mathcal{G}_{c1}} = \{a, b, c, d, e, f, g, h\}$, $V_{\mathcal{G}_{c2}} = \{i, j, k, l, m\}$, and $V_{\mathcal{G}_{c3}} = \{n, o, p, q, r\}$.

Notations: Let $\mathbb{R}$ denote the real field. Vectors are set in boldface lowercase letters, and matrices in boldface capital letters. We write a_i for the ith entry of the vector $\boldsymbol{a}$, and a_{ij} for the (i, j)th entry of the matrix $\boldsymbol{A}$, that is, $a_{ij} = [\boldsymbol{A}]_{i,j}$, such that $\boldsymbol{A} = [a_{ij}]$. Let $\text{diag}(\boldsymbol{A}_1, \ldots, \boldsymbol{A}_k)$ denote a block-diagonal matrix with matrices $\boldsymbol{A}_i$, $1 \leq i \leq k$, being its diagonal entries. Let $\boldsymbol{I}_m$ be the $m \times m$ identity matrix and $\boldsymbol{O}_m$ be the $m \times m$ zero matrix. We use $\mathbf{1}_n \in \mathbb{R}^n$ and $\mathbf{0}_n \in \mathbb{R}^n$ to denote the all-one and all-zero vectors, respectively. The superscript T is the transpose, and $\otimes$ represents the Kronecker product. $\langle \cdot, \cdot \rangle$ denotes the inner product. $\text{tr}(\cdot)$ and $\text{vec}(\cdot)$ are the trace and vectorization operators in linear algebra, respectively. Denote the zero-mean real Gaussian distribution with variance σ^2 by $\mathcal{N}(0, \sigma^2)$.

II. Preliminaries

In this section, we recall the basic definitions and early results of graph theory, algebraic graph theory, time-series analysis, and estimation theory, those which will be used in this study. Please refer to [38]–[41] for more details.

First, consider an undirected graph $\mathcal{G} = (V_{\mathcal{G}}, E_{\mathcal{G}})$, where $V_{\mathcal{G}}$ and $E_{\mathcal{G}}$ denote the sets of vertices and edges, respectively.

Definition: The graph $\mathcal{G}$ is connected if each pair of vertices in $\mathcal{G}$ belongs to a path, and disconnected otherwise. A subgraph of $\mathcal{G}$ is a graph $\mathcal{H} = (V_{\mathcal{H}}, E_{\mathcal{H}})$ such that $V_{\mathcal{H}} \subset V_{\mathcal{G}}$ and $E_{\mathcal{H}} \subset E_{\mathcal{G}}$ [38].

Definition 1 (Component): The *component* of $\mathcal{G}$ is a maximal connected subgraph that is connected and is not contained in any other connected subgraph of $\mathcal{G}$ [38].

Note that to illustrate the concept of components, an example of $\mathcal{G}$ is shown in Fig. 1, where $\mathcal{G}$ is a disconnected graph that has three components.

Proposition 1 [38], [39]: Any two vertices belonging to the same component are connected by at least one path.

Proposition 2 [38], [39]: If $\mathcal{G}$ is a connected graph, it has exactly one component consisting of the whole graph. Otherwise $\mathcal{G}$ has at least two components, which are pairwise disjoint.

Definition (Algebraic Connectivity): Denote the Laplacian matrix of $\mathcal{G}$ by $\mathcal{L}$. Let $\lambda_1, \ldots, \lambda_N$ be the eigenvalues of $\mathcal{L}$, where $\lambda_i \geq 0$ is the ith smallest eigenvalue and λ_2 is the *algebraic connectivity* that indicates the global connectivity of $\mathcal{G}$ [39].

Proposition 3 [13], [31], [39]: Since $\mathcal{G}$ is an undirected graph, $\mathcal{L}$ is symmetric positive semidefinite and there exists an orthogonal matrix $\boldsymbol{U} = \left[(\mathbf{1}_N/\sqrt{N})\ \boldsymbol{Y}_1\right] = [u_{i,j}] \in \mathbb{R}^{N\times N}$ satisfying $\boldsymbol{U}^T\mathcal{L}\boldsymbol{U} = \boldsymbol{\Lambda}$, where $\boldsymbol{\Lambda} = \text{diag}(\lambda_1, \lambda_2, \ldots, \lambda_N)$ is a diagonal matrix whose diagonal entries are the eigenvalues of $\mathcal{L}$, noting that $\lambda_1 \equiv 0$ since $\mathcal{L}\mathbf{1}_N = \mathbf{0}_N$.

Next, let us review some details of the time-series analysis [40]. A time series is a sequence of values of a variable at successive equally spaced points in time, denoted by $\{X_k\}_{k=1}^K$. The time-series analysis consists of methods for analyzing time-series data to extract meaningful features of the data, such as the convergence behavior below.

Definition (Convergence in Probability [40]): Let $\{X_k\}$ be a time series, which is said to *converge in probability* to c if for all $\varepsilon > 0$, $\lim_{k\to\infty} P(|X_k - c| > \varepsilon) = 0$. This is indicated as

$$X_k \xrightarrow{p} c. \tag{1}$$

Definition (Convergence in Distribution [40]): For a time series $\{X_k\}$, let $F_{X_k}(x)$ denote the cumulative distribution function of X_k. If there exists a cumulative distribution function $F_X(x)$ such that $\lim_{k\to\infty} F_{X_k}(x) = F_X(x)$ for every number x at which $F_X(\cdot)$ is continuous, then X_K is said to *converge in distribution* to X, denoted as

$$X_k \xrightarrow{L} X. \tag{2}$$

In deriving the main results of this article, we will be faced with a specific type of time series and its associated testing problem, which are defined as follows.

Definition: A time series $\{Y_k\}_{k=0}^K$ is called a *first-order autoregressive time series [40]*, if it satisfies

$$Y_k = \rho Y_{k-1} + \varepsilon_k, \quad k = 1, \ldots, K \tag{3}$$

where $0 < \rho \leq 1$, Y_0 is a constant, and $\{\varepsilon_k\}_{k=1}^K$ is an i.i.d. white noise sequence with zero mean and variance σ^2. This time series is said to be *unit-root autoregressive* (or called a *unit-root autoregression*) if $\rho = 1$ [40].

Definition (Unit-Root Testing Problem [40]): To test whether the time series (3) is unit-root autoregressive (i.e., $\rho = 1$) based on the data $\{Y_k\}_{k=0}^K$, is the so-called *unit-root testing problem*.

This problem is the starting point of many empirical time-series studies, which can be resolved by using the OLS estimation.[1] The OLS estimation is to find an estimate of the parameter ρ from the sampled data $\{Y_k\}_{k=0}^K$ of the time series (3). For any real valued $0 < \rho \leq 1$, the OLS estimate of ρ can be written as

$$\hat{\rho}_K = \frac{\sum_{k=1}^K Y_k Y_{k-1}}{\sum_{k=1}^K Y_{k-1}^2} \tag{4}$$

which is the maximum-likelihood estimate of ρ conditioned on $\{Y_k\}_{k=0}^K$. We note that there are several useful properties of OLS estimation.

Proposition 4 [40, Proposition 17.1, Example 7.15]: Consider the time series (3), denoted by $\{Y_k\}_{k=0}^K$.

1) If $\{Y_k\}_{k=0}^K$ is unit-root autoregressive, that is, $\rho = 1$, then $([\sum_{k=1}^K Y_{k-1}^2]/K^2) \xrightarrow{L} \sigma^2 \int_0^1 [\mathcal{B}'(s)]^2 ds$ and $([\sum_{k=1}^K Y_{k-1}\varepsilon_k]/K^2) \xrightarrow{p} 0$, where $\mathcal{B}'(s)$ is 1-D Brownian motion.
2) If $\{Y_k\}_{k=0}^K$ is not unit-root autoregressive, that is, $0 < \rho < 1$, then $([\sum_{k=1}^K Y_{k-1}^2]/K) \xrightarrow{p} (\sigma^2/1-\rho^2)$ and $([\sum_{k=1}^K Y_{k-1}\varepsilon_k]/K) \xrightarrow{p} 0$.
3) The estimate $\hat{\rho}_K$ is consistent, that is
$$\hat{\rho}_K \xrightarrow{p} \rho \tag{5}$$
since, by definition, $\hat{\rho}_K = \rho + ([\sum_{k=1}^K Y_{k-1}\varepsilon_k] / [\sum_{k=1}^K Y_{k-1}^2])$.

Based on the OLS estimation, the following decision rule can be used to judge whether the time series $\{Y_k\}_{k=0}^K$ is unit-root autoregressive.

Decision Rule 1: After performing the OLS estimate as (4), the first-order autoregressive time series $\{Y_k\}_{k=0}^K$ is judged to be unit-root autoregressive, if the following condition is satisfied:

$$\left|\hat{\rho}_K - 1\right| \leq C \tag{6}$$

where $C \in (0, 1)$ is a real number.

The unit-root testing problem can be treated as a binary hypothesis-testing problem [41], by assuming that there are two hypotheses, that is, null hypothesis H_0 and alternative hypothesis H_1, which are written as

$$\begin{aligned} H_0 &: \{Y_k\}_{k=0}^K \text{ is } \textit{NOT} \text{ unit-root autoregressive} \\ H_1 &: \{Y_k\}_{k=0}^K \text{ is unit-root autoregressive} \end{aligned} \tag{7}$$

respectively. Therefore, we are able to implement the unit-root testing by using Decision Rule 1 to make decisions, that is, accepting or rejecting H_1, based on the estimated $\hat{\rho}_K$ from the data $\{Y_k\}_{k=0}^K$. The relations between truth and falseness of the decision are illustrated in Table I.

TABLE I
RELATIONS BETWEEN TRUTH AND FALSENESS OF THE DECISION

	H_0 is true	H_1 is true
Reject H_1	Right decision	Wrong decision (Miss)
Accept H_1	Wrong decision (False alarm)	Right decision

A basic measure for the performance evaluation of Decision Rule 1 is the probability of making a wrong decision, called error probability and defined as follows.

Definition (Error Probability [41]): A decision rule for binary hypothesis testing has two types of error probability.

[1] To simplify the analysis, we use OLS estimation in this study. Other methods (such as the Dickey–Fuller test) are able to achieve better performance but making the analysis much more complicated [40].

1) The first type is called *miss probability*, which is the probability that the rule makes a wrong decision, that is, rejecting H_1 when H_1 is true (H_0 is false).
2) The second type is called *false alarm probability*, which is the probability that the rule makes a wrong decision, that is, accepting H_1 when H_1 is false (H_0 is true).

Remark: The miss and false alarm probabilities can be denoted as $P(|\rho^K_{\imath,\ell} - 1| > C|H_1)$ and $P(|\rho^K_{\imath,\ell} - 1| \leq C|H_0)$, respectively.

III. Model

A. Multiagent System

Consider a multiagent system consisting of N_a agents with the second-order dynamics [33]–[35]

$$\dot{\boldsymbol{p}}_i(t) = \boldsymbol{v}_i(t), \quad \dot{\boldsymbol{v}}_i(t) = \boldsymbol{u}_i(t), \quad i = 1, \dots, N_a, \; t \in [0, +\infty) \tag{8}$$

where $\boldsymbol{p}_i(t) \in \mathbb{R}^M$ and $\boldsymbol{v}_i(t) \in \mathbb{R}^M$ are the position and velocity of agent i, respectively, and $\boldsymbol{u}_i(t) \in \mathbb{R}^M$ denotes the control input. Assume that $\boldsymbol{u}_i(t)$ uses the formation-control law as

$$\boldsymbol{u}_i(t) = -\alpha\big(\boldsymbol{v}_i(t) - \boldsymbol{v}^*\big) - \sum_{j=1}^{N_a} g_{ij}\big(\Delta\boldsymbol{p}_{ij}(t) + \beta\Delta\boldsymbol{v}_{ij}(t)\big) \tag{9}$$

where α and β are positive constants satisfying $\alpha\beta > 1$. $\boldsymbol{v}^* \in \mathbb{R}^M$ is the desired velocity. g_{ij} denotes the interagent communication between two agents i and j, that is, $g_{ij} = 1$ if there is a communication link between them and $g_{ij} = 0$ otherwise; while $g_{ii} = 0$ for all $i \in \{1, \dots, N_a\}$. The communication is bidirectional, that is, $g_{ij} = g_{ji}$ for $i \neq j$. In addition

$$\begin{aligned}\Delta\boldsymbol{p}_{ij}(t) &= \big(\boldsymbol{p}_i(t) - \boldsymbol{\delta}_i\big) - \big(\boldsymbol{p}_j(t) - \boldsymbol{\delta}_j + \boldsymbol{\varepsilon}_{i,j,p}\big),\\ \Delta\boldsymbol{v}_{ij}(t) &= \boldsymbol{v}_i(t) - \big(\boldsymbol{v}_j(t) + \boldsymbol{\varepsilon}_{i,j,v}\big)\end{aligned} \tag{10}$$

where $\boldsymbol{\delta}_i \in \mathbb{R}^M$ is the position offset of agent i in the formation, while $\boldsymbol{\varepsilon}_{i,j,p} \in \mathbb{R}^M$ and $\boldsymbol{\varepsilon}_{i,j,v} \in \mathbb{R}^M$ denote the random errors.

Define

$$\boldsymbol{x}_i(t) := \begin{bmatrix}\boldsymbol{p}_i(t) - \boldsymbol{\delta}_i - \boldsymbol{v}^* t\\ \boldsymbol{v}_i(t) - \boldsymbol{v}^*\end{bmatrix}, \quad \boldsymbol{A} := \begin{bmatrix}0 & 1\\ 0 & -\alpha\end{bmatrix} \otimes \boldsymbol{I}_m,$$
$$\boldsymbol{B} := \begin{bmatrix}0\\1\end{bmatrix} \otimes \boldsymbol{I}_m, \qquad \boldsymbol{K} := \begin{bmatrix}-1 & -\beta\end{bmatrix} \otimes \boldsymbol{I}_m. \tag{11}$$

The system (8) can thus be remodeled as [27], [31]

$$\dot{\boldsymbol{x}}_i(t) = \boldsymbol{A}\boldsymbol{x}_i(t) + \boldsymbol{B}\boldsymbol{u}_i(t) \tag{12}$$

$$\boldsymbol{u}_i(t) = \sum_{j=1}^{N_a}\big[g_{ij}\boldsymbol{K}\big(\boldsymbol{x}_i(t) - \boldsymbol{x}_j(t) + \boldsymbol{\varepsilon}_{i,j}(t)\big)\big] \tag{13}$$

where $\boldsymbol{\varepsilon}_{i,j}(t) := \boldsymbol{\varepsilon}_{i,j,p} + \beta\boldsymbol{\varepsilon}_{i,j,v}$. Assume that all elements of $\boldsymbol{\varepsilon}_{i,j}(t)$ are independent white noises [32], [35]; that is, by letting $\varepsilon_{i,j,l}(t)$ be the lth entry of $\boldsymbol{\varepsilon}_{i,j}(t)$, one can have that $\varepsilon_{i,j,l}(t) \sim \mathcal{N}(0, \sigma^2)$ for every i, j, l, and any t, and that $\{\varepsilon_{i,j,l}(t)\}$ are stationary processes, where $\varepsilon_{\imath,j_1,l_1}(t_1)$ and $\varepsilon_{\ell,j_2,l_2}(t_2)$ are independent for $\imath \neq \ell$, $j_1 \neq j_2$, $l_1 \neq l_2$, or $t_1 \neq t_2$.

Remark 1: For clarity of presentation, we focus on investigating multiagent systems using the formation-control law described by (9) and (10). In fact, the derived results should apply to multiagent systems with various control laws as long as the systems can be remodeled by (12) and (13), where (12) is a classic dynamics model for multiagent systems and (13) is a typical consensus-control input with noise [27], [45].

We now specify the communication graph of the system as follows [13], [34], [38]. Let $V_a = \{1, \dots, N_a\}$ be the set of N_a agents with $i \in V_a$ representing agent i. The graph $\mathcal{G}_a = (V_a, E_a)$ is used to model the interagent communications among the agents, where $\mathcal{G}_a$ is an undirected graph and $E_a \in V_a \times V_a$ is the edge set of paired agents. An edge $(j, i) \in E_a$ implies that agent i can straightforwardly communicate with agent j, that is, $g_{ij} = 1$. The *Laplacian matrix* of $\mathcal{G}_a$ can be written as $\mathcal{L}_a = [l_{ij}]$, where $l_{ii} = \sum_{j\neq i} g_{ij}$ and $l_{ij} = -g_{ij}$ for $i \neq j$. Since this study considers the disconnected network scenario, we make the following assumption.

Assumption 1: The communication graph $\mathcal{G}_a$ is a disconnected graph.

This assumption means that $\mathcal{G}_a$ has more than one component, under which we are interested in monitoring the connectivity between two arbitrarily chosen agents. This type of connectivity is especially useful for showing precise system status and helping to remerge the multiagent system when $\mathcal{G}_a$ is a disconnected graph.

Without loss of generality, suppose that agents $\imath$ and ℓ are the two agents of interest. The formal definition of the connectivity between two agents is given as follows.

Definition 2 (Connected and Disconnected Agents): Agents $\imath$ and ℓ are said to be *connected* if there is a path between vertices $\imath$ and ℓ in graph $\mathcal{G}_a$, and *disconnected* otherwise.

B. External Estimator

We are concerned with identifying the disconnectedness between two arbitrarily chosen agents (denoted by agents $\imath$ and ℓ) in multiagent systems via external estimators.[2] Assume that there is an external estimator monitoring the connection status of agents $\imath$ and ℓ in the multiagent system (8). The agents and external estimator have their own tasks to perform.

1) Agents $\imath$ and ℓ take the samples of $\boldsymbol{x}_\imath(t)$ and $\boldsymbol{x}_\ell(t)$ at $t = k\tau$, respectively, with a sampling interval of τ, and then transmit the sampled data $\boldsymbol{x}_\imath(k\tau)$ and $\boldsymbol{x}_\ell(k\tau)$ to the external estimator via long-range communication links,[3] where $k = 0, 1, \dots, K$ and K is the number of data samples.
2) After receiving the sampled data $\boldsymbol{x}_\imath(k\tau)$ and $\boldsymbol{x}_\ell(k\tau)$, $k = 0, 1, \dots, K$, from agents $\imath$ and ℓ, respectively, the external estimator first computes

$$\boldsymbol{d}_{\imath,\ell}[k] = \boldsymbol{x}_\imath(k\tau) - \boldsymbol{x}_\ell(k\tau) \tag{14}$$

[2]External estimators are used to monitor agents' statuses, which typically exist in control stations that provide facilities for external (human) supervision and regulation of a multiagent system, for example, ground control centers and manned vehicles for a multi-UAV system [28], [30]. See Fig. 2 for an illustration.

[3]Within a multiagent system, in addition to the interagent communications, there are long-range communication links between the agents and the control station in general, so that agents can communicate with the control station on demand. These long-range communications are independent of the interagent communications and cannot replace them, because the long-range communications are relatively costly. See Fig. 2 for an illustration.

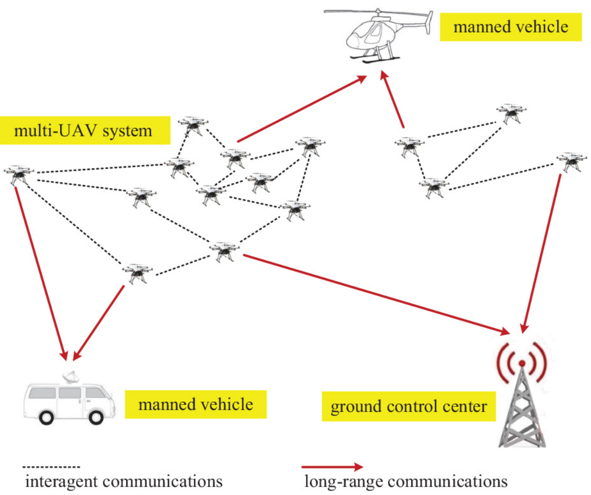

Fig. 2. Multiagent system (i.e., a multi-UAV system) with control stations that have external estimators. Control stations can be ground control centers and manned vehicles. Note that the long-range communications are independent with the interagent communications.

and then estimates

$$\rho_{\imath,\ell}^K = \frac{\sum_{k=1}^K \langle \boldsymbol{d}_{\imath,\ell}[k], \boldsymbol{d}_{\imath,\ell}[k-1] \rangle}{\sum_{k=1}^K \langle \boldsymbol{d}_{\imath,\ell}[k-1], \boldsymbol{d}_{\imath,\ell}[k-1] \rangle}. \quad (15)$$

Note that $\rho_{\imath,\ell}^K$ is an OLS-type estimate that requires inner product $\langle \cdot, \cdot \rangle$ since $\boldsymbol{d}_{\imath,\ell}[k]$ and $\boldsymbol{d}_{\imath,\ell}[k-1]$ are vectors, while the classical OLS estimate in time-series theory involves only the product of two real numbers [40] [see (4)].

Then, identifying the disconnectedness between agents $\imath$ and ℓ can be treated as binary hypothesis testing. Specifically, we assume that there are two hypotheses

$$H_0 : \text{Agents } \imath \text{ and } \ell \text{ are connected,} \quad (16)$$

$$H_1 : \text{Agents } \imath \text{ and } \ell \text{ are disconnected} \quad (17)$$

and design the decision rule as follows.

Decision Rule 2: Agents $\imath$ and ℓ are judged to be disconnected (i.e., accepting H_1), if the following condition is satisfied:

$$\left|\rho_{\imath,\ell}^K - 1\right| \le C \quad (18)$$

where K is the number of data samples, and $C \in (0, 1)$.

The formulation of this rule is inspired by Decision Rule 1 for the unit-root testing problem of the first-order autoregressive time series. Obviously both the estimate and decision have low complexity, because (14) and (15) require MK subtractions, $2MK$ multiplications, $2MK$ additions, and 1 division. We propose to set $C = 0.5$ since 0.5 is the median of 0 and 1, noting that this setting will be checked in the simulation.

The exact expressions for τ and K are not yet available due to the absence of *a prior* information about the communication graph $\mathcal{G}_a$ at the external estimator. Therefore, we propose a best-effort procedure to identify disconnected agents, which is described by Procedure 1. The procedure uses progressively increasing τ as long as there is plenty of time. That is why it is called the best-effort procedure. In line 3 of Procedure 1, $f(\tau_0, T)$ is a positive monotonically increasing function of T.

Procedure 1: Best-Effort Procedure to Identify Disconnected Agents

1 Initialize positive real parameter τ_0 and positive integer parameter K, and set $T = 1$ at external estimator;
2 **while** *There is plenty of time* **do**
3 External estimator computes parameter $\tau = f(\tau_0, T)$; `// f(τ0, T) is a monotonically increasing function of T, e.g.,` $f(\tau_0, T) = \tau_0 T$
4 External estimator sends τ and K to agents $\imath$ and ℓ;
5 Agents $\imath$ and ℓ take new samples and transmit the sampled data $\boldsymbol{x}_\imath(k\tau)$ and $\boldsymbol{x}_\ell(k\tau)$, $k = 0, 1, \cdots, K$, to external estimator;
6 External estimator estimates $\rho_{\imath,\ell}^K$ and uses Decision Rule 2 to make a decision;
7 $T = T + 1$;
8 **end**

For example, we will set $f(\tau_0, T) = \tau_0 T$ in the simulation. Besides, we propose to select K as large as possible while the simulation results (Figs. 8–10) will show that setting $10 \le K \le 20$ might be large enough for many cases.

To evaluate the performance of Decision Rule 2, we will also use the measure of error probability in our analysis.

Remark 2: The miss probability of Decision rule 2 is the probability of event $|\rho_{\imath,\ell}^K - 1| > C$ under the hypothesis that agents $\imath$ and ℓ are disconnected (i.e., H_1), which is written as

$$P\left(\left|\rho_{\imath,\ell}^K - 1\right| > C|\text{Disconnected}\right) = P\left(\left|\rho_{\imath,\ell}^K - 1\right| > C|H_1\right) \quad (19)$$

and the false alarm probability is the probability of event $|\rho_{\imath,\ell}^K - 1| \le C$ under the hypothesis that agents $\imath$ and ℓ are connected (i.e., H_0), which is written as

$$P\left(\left|\rho_{\imath,\ell}^K - 1\right| \le C|\text{Connected}\right) = P\left(\left|\rho_{\imath,\ell}^K - 1\right| \le C|H_0\right). \quad (20)$$

Note that the definitions of H_1 and H_0 can be found in (17) and (16), respectively. Obviously, the miss and false alarm probabilities are the probabilities of Decision Rule 2 making a wrong decision under the conditions that agents $\imath$ and ℓ are disconnected and connected, respectively.

IV. Analysis

This section is dedicated to the analysis of identifying disconnected agents with Decision Rule 2 and Procedure 1. We will first give useful lemmas and then present the derived results, for which detailed proofs will be provided in an independent section at the end.

A. Useful Lemmas

For the multiagent system (8), we adopt the concept of components in graph theory to describe and analyze the communication graph $\mathcal{G}_a$ that is a disconnected graph (see Assumption 1).

Definition 3: Suppose that agent $\imath$ belongs to component $\mathcal{G}_\imath$ of the communication graph $\mathcal{G}_a$ and agent ℓ belongs to component $\mathcal{G}_\ell$, that is, $\imath \in V_{\mathcal{G}_\imath}$ and $\ell \in V_{\mathcal{G}_\ell}$. Define

$$\widetilde{\mathcal{G}}_{\imath\ell} := \mathcal{G}_\imath \cup \mathcal{G}_\ell \tag{21}$$

such that $\mathcal{G}_\imath, \mathcal{G}_\ell \subseteq \widetilde{\mathcal{G}}_{\imath\ell} \subseteq \mathcal{G}_a$. Assume that $\widetilde{\mathcal{G}}_{\imath\ell}$ has N vertices, that is, $V_{\widetilde{\mathcal{G}}_{\imath\ell}} = \{i_1, \dots, i_N\}$. That is, there are N agents, denoted by $i_1, \dots, i_N$, belonging to $\widetilde{\mathcal{G}}_{\imath\ell}$, where $N \le N_a$.

Remark 3: By definition, it is known that $\widetilde{\mathcal{G}}_{\imath\ell}$ has at most two components. That is, when $\mathcal{G}_\imath$ and $\mathcal{G}_\ell$ are disjoint (i.e., $\mathcal{G}_\imath \cap \mathcal{G}_\ell = \emptyset$), $\widetilde{\mathcal{G}}_{\imath\ell}$ consists of two components, implying that agents $\imath$ and ℓ are disconnected.

Under Assumption 1, the communication graph $\mathcal{G}_a$ is disconnected, while agents $\imath$ and ℓ are either disconnected or connected.

Lemma 1: The following statements are equivalent.
1) Agents $\imath$ and ℓ are disconnected.
2) $\widetilde{\mathcal{G}}_{\imath\ell}$ has two components, that is, $\mathcal{G}_\imath$ and $\mathcal{G}_\ell$, such that agents $\imath$ and ℓ belong to two disjoint components (i.e., $\mathcal{G}_\imath$ and $\mathcal{G}_\ell$ satisfy $\mathcal{G}_\imath \cap \mathcal{G}_\ell = \emptyset$).
3) $\lambda_1 = \lambda_2 = 0$, and $\lambda_i > 0$ for all $i = 3, \dots, N$.

Accordingly, the following statements are also equivalent.
1) Agents $\imath$ and ℓ are connected.
2) $\widetilde{\mathcal{G}}_{\imath\ell}$ consists of only one component, such that agents $\imath$ and ℓ belong to the same component (i.e., $\mathcal{G}_\imath = \mathcal{G}_\ell$).
3) $\lambda_1 = 0$, and $\lambda_i > 0$ for all $i = 2, \dots, N$.

According to this lemma, it is always true that $\lambda_1 = 0$ and $\lambda_i > 0$ with $i = 3, \dots, N$. However, the value of λ_2 is different in two cases, that is, $\lambda_2 > 0$ if agents $\imath$ and ℓ are connected, and $\lambda_2 = 0$ if they are disconnected. Note that Fig. 3(a) and (b) illustrates Definition 3, Remark 3, and Lemma 1.

Lemma 2: With $\boldsymbol{A}$, $\boldsymbol{B}$, and $\boldsymbol{K}$ being defined in (11), if $\alpha > 0$, $\beta > 0$, and $\alpha\beta > 1$, then for each $\lambda_i \ge 0$, we have

$$\boldsymbol{A} + \lambda_i \boldsymbol{B}\boldsymbol{K} = \begin{bmatrix} 0 & 1 \\ -\lambda_i & -(\alpha + \beta\lambda_i) \end{bmatrix} \otimes \boldsymbol{I}_M = \boldsymbol{\Theta}_i \boldsymbol{\Phi}_i \boldsymbol{\Theta}_i^{-1} \tag{22}$$

where

$$\boldsymbol{\Theta}_i = \begin{bmatrix} 1 & 1 \\ -\frac{\alpha+\beta\lambda_i}{2} + \sqrt{\frac{(\alpha+\beta\lambda_i)^2}{4} - \lambda_i} & -\frac{\alpha+\beta\lambda_i}{2} - \sqrt{\frac{(\alpha+\beta\lambda_i)^2}{4} - \lambda_i} \end{bmatrix} \otimes \boldsymbol{I}_M$$

$$\boldsymbol{\Phi}_i = \begin{bmatrix} -\frac{\alpha+\beta\lambda_i}{2} + \sqrt{\frac{(\alpha+\beta\lambda_i)^2}{4} - \lambda_i} & 0 \\ 0 & -\frac{\alpha+\beta\lambda_i}{2} - \sqrt{\frac{(\alpha+\beta\lambda_i)^2}{4} - \lambda_i} \end{bmatrix} \otimes \boldsymbol{I}_M$$

$$\boldsymbol{\Theta}_i^{-1} = -\frac{1}{2\sqrt{\frac{(\alpha+\beta\lambda_i)^2}{4} - \lambda_i}} \begin{bmatrix} -\frac{\alpha+\beta\lambda_i}{2} - \sqrt{\frac{(\alpha+\beta\lambda_i)^2}{4} - \lambda_i} & -1 \\ \frac{\alpha+\beta\lambda_i}{2} - \sqrt{\frac{(\alpha+\beta\lambda_i)^2}{4} - \lambda_i} & 1 \end{bmatrix} \otimes \boldsymbol{I}_M.$$

We now focus on $\boldsymbol{\Phi}_i$, especially on $\boldsymbol{\Phi}_2$, recalling that the value of λ_2 can be used to distinguish whether agents $\imath$ and ℓ are connected or not (see Lemma 1).

Lemma 3: Denote $\boldsymbol{\Phi}_i = \mathrm{diag}(\phi_{i,1}, \dots, \phi_{i,2M})$.
1) If agents $\imath$ and ℓ are disconnected such that $\lambda_2 = 0$, then $\phi_{2,1} = \cdots = \phi_{2,M} = 0$. Otherwise, $\lambda_2 > 0$, and $\phi_{2,1} = \cdots = \phi_{2,M} < 0$.
2) $\phi_{2,M+1} = \cdots = \phi_{2,2M} < 0$.
3) $\phi_{i,1} = \cdots = \phi_{i,2M} < 0$ for all $i = 3, \dots, N$.

B. Main Results

The communication graph $\mathcal{G}_a$ of the multiagent system (8) is a disconnected graph under Assumption 1. According to Proposition 2, the states of N agents belonging to $\widetilde{\mathcal{G}}_{\imath\ell}$ [defined in (21)] are not affected by agents in components other than $\mathcal{G}_\imath$ and $\mathcal{G}_\ell$.

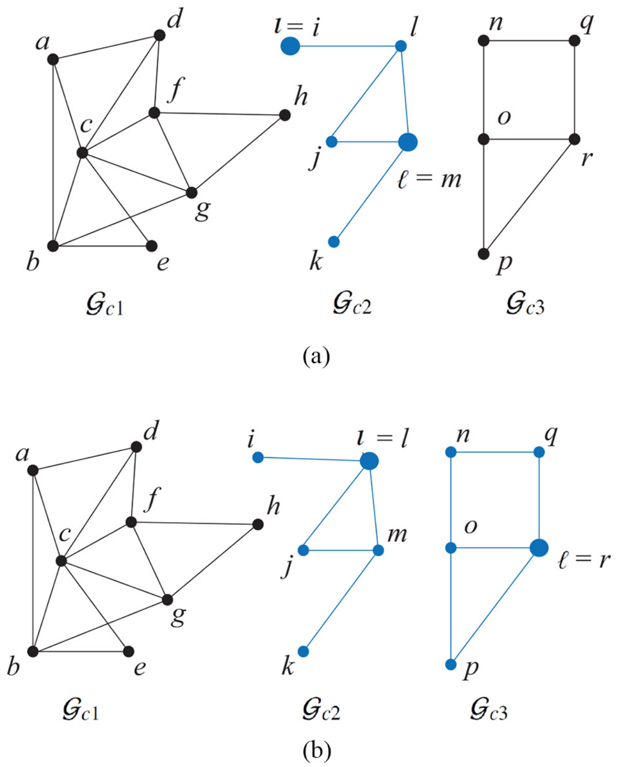

Fig. 3. Two examples of $\widetilde{\mathcal{G}}_{\imath\ell} = \mathcal{G}_\imath \cup \mathcal{G}_\ell$, when the communication graph $\mathcal{G}_a$ has three components (i.e., $\mathcal{G}_{c1}$, $\mathcal{G}_{c2}$, and $\mathcal{G}_{c3}$) such that $\mathcal{G}_a = \mathcal{G}_{c1} \cup \mathcal{G}_{c2} \cup \mathcal{G}_{c3}$. It is easy to see that $\widetilde{\mathcal{G}}_{\imath\ell} = \mathcal{G}_\imath \cup \mathcal{G}_\ell \subset \mathcal{G}_a$. For clarity, $\widetilde{\mathcal{G}}_{\imath\ell}$ is shown in blue. (a) If agents $\imath$ and ℓ belong to the same component (i.e., $\imath = i \in V_{\mathcal{G}_{c2}}$ and $\ell = m \in V_{\mathcal{G}_{c2}}$), then $\widetilde{\mathcal{G}}_{\imath\ell} = \mathcal{G}_\imath = \mathcal{G}_\ell = \mathcal{G}_{c2}$ has only one component and thus two agents are connected. (b) If agents $\imath$ and ℓ belong to two disjoint components (i.e., $\imath = l \in V_{\mathcal{G}_{c2}}$ and $\ell = r \in V_{\mathcal{G}_{c3}}$), then $\widetilde{\mathcal{G}}_{\imath\ell} = \mathcal{G}_\imath \cup \mathcal{G}_\ell = \mathcal{G}_{c2} \cup \mathcal{G}_{c3}$ consists of two components (i.e., $\mathcal{G}_{c2}$ and $\mathcal{G}_{c3}$), and thus two agents are disconnected.

Therefore, the forthcoming analysis can be restricted to N agents that belong to $\widetilde{\mathcal{G}}_{\imath\ell}$, that is, agents $i_1, \dots, i_N$. Thus, let $\boldsymbol{x}(t) := [\boldsymbol{x}_{i_1}^T(t), \dots, \boldsymbol{x}_{i_N}^T(t)]^T$ and $\boldsymbol{\varepsilon}(t) := [\boldsymbol{\varepsilon}_{i_1}^T(t), \dots, \boldsymbol{\varepsilon}_{i_N}^T(t)]^T$, where $\boldsymbol{\varepsilon}_i(t) := [\boldsymbol{\varepsilon}_{i,1}^T(t), \dots, \boldsymbol{\varepsilon}_{i,N}^T(t)]^T$. Combining them with (12) and (13) yields [31, eq. (4)], [32, eq. (4)]

$$\dot{\boldsymbol{x}}(t) = (\boldsymbol{I}_N \otimes \boldsymbol{A} + \mathcal{L} \otimes \boldsymbol{B}\boldsymbol{K})\boldsymbol{x}(t) + (\boldsymbol{G} \otimes \boldsymbol{B}\boldsymbol{K})\boldsymbol{\varepsilon}(t) \tag{23}$$

where $\mathcal{L}$ is given in the definition of algebraic connectivity and $\boldsymbol{G} = \mathrm{diag}(\boldsymbol{g}_{i_1}, \dots, \boldsymbol{g}_{i_N})$ with $\boldsymbol{g}_i = [g_{i,1}, \dots, g_{i,N}]$.

With $\boldsymbol{U}$ and $\boldsymbol{Y}_1$ given in Proposition 3, we define [31], [32]

$$\underline{\boldsymbol{\xi}}(t) := \left(\boldsymbol{U}^T \otimes \boldsymbol{I}_{2M}\right)\left[\left(\boldsymbol{I}_N - \frac{1}{N}\boldsymbol{1}_N\boldsymbol{1}_N^T\right) \otimes \boldsymbol{I}_{2M}\right]\boldsymbol{x}(t) \tag{24}$$

and rewrite the model (23) as [31, eq. (6)]

$$\dot{\underline{\boldsymbol{\xi}}}(t) = (\boldsymbol{I}_N \otimes \boldsymbol{A} + \boldsymbol{\Lambda} \otimes \boldsymbol{B}\boldsymbol{K})\underline{\boldsymbol{\xi}}(t) + \left[\begin{bmatrix} \boldsymbol{0}_N^T \\ \boldsymbol{Y}_1^T\boldsymbol{G} \end{bmatrix} \otimes \boldsymbol{B}\boldsymbol{K}\right]\boldsymbol{\varepsilon}(t).$$

Then, we write $\underline{\boldsymbol{\xi}}(t) = [\underline{\boldsymbol{\xi}}_1^T(t), \dots, \underline{\boldsymbol{\xi}}_N^T(t)]^T$ with $\underline{\boldsymbol{\xi}}_l(t) \in \mathbb{R}^{2M}$, and obtain $\underline{\boldsymbol{\xi}}_1(t) \equiv \boldsymbol{0}_{2M}$ [31]. By defining $\boldsymbol{\zeta}_l(t) := \underline{\boldsymbol{\xi}}_{l+1}(t)$ and $\boldsymbol{\zeta}(t) := [\boldsymbol{\zeta}_1^T(t), \dots, \boldsymbol{\zeta}_{N-1}^T(t)]^T$, we obtain

$$\dot{\boldsymbol{\zeta}}(t) = \underline{\boldsymbol{A}}\boldsymbol{\zeta}(t) + \underline{\boldsymbol{B}}\boldsymbol{\varepsilon}(t) \tag{25}$$

where $\underline{\boldsymbol{A}} = \boldsymbol{I}_{N-1} \otimes \boldsymbol{A} + \boldsymbol{\Lambda}_1 \otimes \boldsymbol{BK}$ with $\boldsymbol{\Lambda}_1 = \mathrm{diag}(\lambda_2, \dots, \lambda_N)$, and $\underline{\boldsymbol{B}} = \boldsymbol{Y}_1^T \boldsymbol{G} \otimes \boldsymbol{BK}$. From Lemma 2, it follows that $\underline{\boldsymbol{A}} = \boldsymbol{Q}\widehat{\boldsymbol{A}}\boldsymbol{Q}^{-1}$, where $\boldsymbol{Q} = \mathrm{diag}(\boldsymbol{\Theta}_2, \dots, \boldsymbol{\Theta}_N)$, $\widehat{\boldsymbol{A}} = \mathrm{diag}(\boldsymbol{\Phi}_2, \dots, \boldsymbol{\Phi}_N)$, and $\boldsymbol{Q}^{-1} = \mathrm{diag}(\boldsymbol{\Theta}_2^{-1}, \dots, \boldsymbol{\Theta}_N^{-1})$.

After defining $\boldsymbol{\eta}_n(t) := \boldsymbol{\Theta}_{n+1}^{-1}\boldsymbol{\zeta}_n(t)$, $n \in \{1, \dots, N-1\}$, we can deduce from (25) that

$$\dot{\boldsymbol{\eta}}_n(t) = \boldsymbol{\Phi}_{n+1}\boldsymbol{\eta}_n(t) + (\boldsymbol{c}(n) \otimes \boldsymbol{I}_{2M})\boldsymbol{Q}^{-1}\underline{\boldsymbol{B}}\boldsymbol{\varepsilon}(t) \tag{26}$$

where $\boldsymbol{c}(n) = [c_1(n), \dots, c_N(n)] \in \mathbb{R}^{1\times N}$ with $c_i(n) = 1$ if $i = n$ and $c_i(n) = 0$ if $i \neq n$. This further yields

$$\boldsymbol{\eta}_n(t) = e^{\boldsymbol{\Phi}_{n+1}t}\boldsymbol{\eta}_n(0) + \\ + \sigma \int_0^t e^{\boldsymbol{\Phi}_{n+1}(t-s)}(\boldsymbol{c}(n) \otimes \boldsymbol{I}_{2M})\boldsymbol{Q}^{-1}\underline{\boldsymbol{B}}d\mathcal{B}(s) \tag{27}$$

where $\mathcal{B}(s) = [\mathcal{B}_1(s), \dots, \mathcal{B}_{2MN^2}(s)]^T$ is $2MN^2$-D Brownian motion [42]. Denoting the qth entry of $\mathcal{B}(s)$ by $\mathcal{B}_q(t)$, we have $d\mathcal{B}_q(s) = ([\varepsilon_q(t)]/\sigma)dt$ [43].

Now, we can obtain the following results.

Lemma 4: Suppose that $\boldsymbol{\eta}_n(t) = [\eta_{n,1}(t)\ \dots,\ \eta_{n,2M}(t)]^T$. Let $\eta_{n,m,k} := \eta_{n,m}(k\tau)$, where $k = 0, \dots, K$. Then, for any $n \in \{1, \dots, N-1\}$ and any $m \in \{1, \dots, 2M\}$, $\{\eta_{n,m,k}\}_{k=0}^K$ is a first-order autoregressive time series as

$$\eta_{n,m,k} = e^{\phi_{n+1,m}\tau}\eta_{n,m,k-1} + \widetilde{\varepsilon}_{n,m,k} \tag{28}$$

where $\widetilde{\varepsilon}_{n,m,k}$ is Gaussian with zero mean, whose definition is given by (40). In particular, $\{\eta_{n,m,k}\}_{k=0}^K$ is unit-root autoregressive if $\phi_{n+1,m} = 0$ such that $e^{\phi_{n+1,m}\tau} = 1$.

Lemma 5: Let $\boldsymbol{\eta}_n[k] := [\eta_{n,1,k}\ \dots,\ \eta_{n,2M,k}]^T$, where $\eta_{n,m,k}$ is defined in Lemma 4. For the external estimator, we have

$$\boldsymbol{d}_{\imath,\ell}[k] = \sum_{n=1}^{N-1}\left(u_{\imath,n+1} - u_{\ell,n+1}\right)\boldsymbol{\Theta}_{n+1}\boldsymbol{\eta}_n[k] \tag{29}$$

where $u_{i,j}$ is the (i, j)th entry of $\boldsymbol{U}$ defined in Proposition 3.

It is worth pointing out that after using the methods of consensus analysis [31], [32], Lemma 5 bridges $\boldsymbol{d}_{\imath,\ell}[k]$ to autoregressive time series, that is, every entry of $\boldsymbol{d}_{\imath,\ell}[k]$ can be regarded as a linear function of $\eta_{n,m,k}$, $n \in \{1, \dots, N-1\}$, $m \in \{1, \dots, 2M\}$, where each $\{\eta_{n,m,k}\}_{k=0}^K$ is a first-order autoregressive time series.

Lemma 6: Suppose that Assumption 1 holds. Let $\widetilde{u}_{n_1,n_2} = (u_{\imath,n_1+1} - u_{\ell,n_1+1})(u_{\imath,n_2+1} - u_{\ell,n_2+1})$. If agents $\imath$ and ℓ are disconnected, then (30)–(33) hold, as shown at the bottom of the page.

This lemma is useful in the computation of $\rho_{\imath,\ell}^K$, since

$$\rho_{\imath,\ell}^K = \frac{\sum_{k=1}^K \langle \boldsymbol{d}_{\imath,\ell}[k], \boldsymbol{d}_{\imath,\ell}[k-1]\rangle}{K^2} \\ \times \left(\frac{\sum_{k=1}^K \langle \boldsymbol{d}_{\imath,\ell}[k-1], \boldsymbol{d}_{\imath,\ell}[k-1]\rangle}{K^2}\right)^{-1} \tag{34}$$

which can further make use of (30)–(33).

Theorem 1: Suppose that Assumption 1 holds. Let $\widetilde{\eta}_{1,i} = ([\sum_{k=1}^K \eta_{1,i,k-1}^2]/K^2)$. If agents $\imath$ and ℓ are disconnected, then

$$\frac{\sum_{k=1}^K \langle \boldsymbol{d}_{\imath,\ell}[k], \boldsymbol{d}_{\imath,\ell}[k-1]\rangle}{K^2} \xrightarrow{p} \widetilde{u}_{1,1}\sum_{i=1}^M \widetilde{\eta}_{1,i} \tag{35}$$

$$\frac{\sum_{k=1}^K \langle \boldsymbol{d}_{\imath,\ell}[k-1], \boldsymbol{d}_{\imath,\ell}[k-1]\rangle}{K^2} \xrightarrow{p} \widetilde{u}_{1,1}\sum_{i=1}^M \widetilde{\eta}_{1,i} \tag{36}$$

such that

$$\rho_{\imath,\ell}^K \xrightarrow{p} 1. \tag{37}$$

Moreover, for each $i \in \{1, \dots, M\}$, $\widetilde{\eta}_{1,i} \xrightarrow{L} \sigma_{m,n}^2 \int_0^1 [\mathcal{B}'(s)]^2 ds$, where $\mathcal{B}'(s)$ is 1-D Brownian motion, and the definition of $\sigma_{m,n}^2$ is given by (44).

By Theorem 1, we can explain why Decision Rule 2 can effectively identify the disconnectedness between agents $\imath$ and ℓ; that is, if two agents are disconnected, for sufficiently large K, $\rho_{\imath,\ell}^K$ will be close enough to 1 such that (18) will certainly be satisfied. This means that the miss probability can be kept arbitrarily small, as precisely pointed out in the following theorem.

Theorem 2: Let Assumption 1 hold. If agents $\imath$ and ℓ are disconnected, then for any $C \in (0, 1)$, the miss probability converges to 0 as K increases, that is

$$\lim_{K\to\infty} P\left(\left|\rho_{\imath,\ell}^K - 1\right| > C|\text{Disconnected}\right) = 0. \tag{38}$$

This theorem describes the convergence behavior of the miss probability. Elegant theoretical results for the false alarm probability of Decision Rule 2 are, however, still beyond analytical reach because analyzing $\rho_{\imath,\ell}^K$ is complicated when agents $\imath$ and ℓ are connected. To gain further insights into the false alarm probability, simulations will be carried out in Section V. Before that, let us provide some comments helpful to understanding the behavior of the false alarm probability.

$$\frac{\sum_{k=1}^K \langle \boldsymbol{d}_{\imath,\ell}[k], \boldsymbol{d}_{\imath,\ell}[k-1]\rangle}{K^2} = \sum_{n_1=1}^{N-1}\sum_{n_2=1}^{N-1}\widetilde{u}_{n_1,n_2}\mathrm{vec}\left(\boldsymbol{\Theta}_{n_1+1}^T\boldsymbol{\Theta}_{n_2+1}\right)^T\mathrm{vec}\left(\frac{\sum_{k=1}^K \boldsymbol{\eta}_{n_2}[k]\left(\boldsymbol{\eta}_{n_1}[k-1]\right)^T}{K^2}\right) \tag{30}$$

$$\xrightarrow{p} \sum_{n_1=1}^{N-1}\sum_{n_2=1}^{N-1}\widetilde{u}_{n_1,n_2}\mathrm{vec}\left(\boldsymbol{\Theta}_{n_1+1}^T\boldsymbol{\Theta}_{n_2+1}\right)^T\mathrm{vec}\left(e^{\boldsymbol{\Phi}_{n_2+1}\tau}\frac{\sum_{k=1}^K \boldsymbol{\eta}_{n_2}[k-1]\left(\boldsymbol{\eta}_{n_1}[k-1]\right)^T}{K^2}\right) \tag{31}$$

$$= \sum_{n_1=1}^{N-1}\sum_{n_2=1}^{N-1}\widetilde{u}_{n_1,n_2}\mathrm{vec}\left(\boldsymbol{\Theta}_{n_1+1}^T\boldsymbol{\Theta}_{n_2+1}\right)^T\left(\boldsymbol{I}_{2M} \otimes e^{\boldsymbol{\Phi}_{n_2+1}\tau}\right)\mathrm{vec}\left(\frac{\sum_{k=1}^K \boldsymbol{\eta}_{n_2}[k-1]\left(\boldsymbol{\eta}_{n_1}[k-1]\right)^T}{K^2}\right) \tag{32}$$

$$\frac{\sum_{k=1}^K \langle \boldsymbol{d}_{\imath,\ell}[k-1], \boldsymbol{d}_{\imath,\ell}[k-1]\rangle}{K^2} = \sum_{n_1=1}^{N-1}\sum_{n_2=1}^{N-1}\widetilde{u}_{n_1,n_2}\mathrm{vec}\left(\boldsymbol{\Theta}_{n_1+1}^T\boldsymbol{\Theta}_{n_2+1}\right)^T\mathrm{vec}\left(\frac{\sum_{k=1}^K \boldsymbol{\eta}_{n_2}[k-1]\left(\boldsymbol{\eta}_{n_1}[k-1]\right)^T}{K^2}\right) \tag{33}$$

Remark 4: Under the condition that agents $\imath$ and ℓ are connected, it can be known that:

1) the convergence as in (37) is generally not valid in this case. Because the expressions in the right-hand sides of equalities in (32) and (33) only differ by the additional term $\boldsymbol{I}_{2M} \otimes e^{\boldsymbol{\Phi}_{n_2+1}\tau}$ in (32) while this term causes $\rho_{\imath,\ell}^{K}$ to deviate from 1. Note that $\boldsymbol{I}_{2M} \otimes e^{\boldsymbol{\Phi}_{n_2+1}\tau}$ is a diagonal matrix whose diagonal entries consist of $e^{\phi_{n+1,m}\tau}$, $n \in \{1, \ldots, N-1\}$, $m \in \{1, \ldots, 2M\}$. For all n and all m, we have $e^{\phi_{n+1,m}\tau} < 1$ such that $e^{\phi_{n+1,m}\tau} \neq 1$;
2) as $\tau \to \infty$, each diagonal entry of $\boldsymbol{I}_{2M} \otimes e^{\boldsymbol{\Phi}_{n_2+1}\tau}$ decreases exponentially to 0, since $\phi_{n+1,m} < 0$. Thus, with ever-increasing τ, $\rho_{\imath,\ell}^{K}$ tends to 0, making the false alarm probability, that is, $P(|\rho_{\imath,\ell}^{K} - 1| \leq C|\text{Connected})$, to decrease. This means that Procedure 1 should be able to substantially reduce the false alarm probability, which will be shown in the simulation (Section V).

C. Proofs

The proofs of the derived results are provided as follows.

Proof of Lemma 1: Equivalence of 1) and 2) follows from Propositions 1 and 2. On the other hand, 3) is equivalent to 1) and 2), because the multiplicity of the eigenvalue 0 of $\mathcal{L}$ equals the number of components [37]. To be specific, if $\widetilde{\mathcal{G}}_{\imath\ell}$ has only one component, then the multiplicity is 1 such that $\lambda_1 = 0$ and $\lambda_i > 0$ for all $i = 2, \ldots, N$; if $\widetilde{\mathcal{G}}_{\imath\ell}$ has two components, then the multiplicity is 2 such that $\lambda_1 = \lambda_2 = 0$ and $\lambda_i > 0$ for all $i = 3, \ldots, N$. ∎

Proof of Lemma 2: Verifying (22) just requires direct multiplication of the matrices $\boldsymbol{\Theta}_i$, $\boldsymbol{\Phi}_i$, and $\boldsymbol{\Theta}_i^{-1}$. ∎

Proof of Lemma 3: It is easy to check this result by substituting $\lambda_i = 0$ or $\lambda_i > 0$ into $\boldsymbol{\Phi}_i$ (defined in Lemma 2). That is, since $\alpha, \beta > 0$ and $\alpha\beta > 1$, if $\lambda_i = 0$, we have $\boldsymbol{\Phi}_i = \begin{bmatrix} 0 & 0 \\ 0 & -\alpha \end{bmatrix} \otimes \boldsymbol{I}_M$; then if $\lambda_i > 0$, $-([\alpha + \beta\lambda_i]/2) - \sqrt{([(\alpha + \beta\lambda_i)^2]/4) - \lambda_i} < 0$ and $-([\alpha + \beta\lambda_i]/2) + \sqrt{([(\alpha + \beta\lambda_i)^2]/4) - \lambda_i} = -(\lambda_i/[(\alpha + \beta\lambda_i/2) + \sqrt{((\alpha + \beta\lambda_i)^2/4) - \lambda_i}]) < 0$. ∎

Proof of Lemma 4: Let $\boldsymbol{c}'(m) = [c_1'(m), \ldots, c_{2M}'(m)] \in \mathbb{R}^{1\times 2M}$, where $c_\jmath'(m) = 1$ if $\jmath = m$ and $c_\jmath'(m) = 0$ if $\jmath \neq m$. Suppose that $\boldsymbol{\varepsilon}(t) = [\varepsilon_1(t), \ldots, \varepsilon_{2N^2M}(t)]^T \in \mathbb{R}^{2N^2M}$. From (26), we have

$$\begin{aligned} \dot{\eta}_{n,m}(t) &= \phi_{n+1,m}\eta_{n,m}(t) + \boldsymbol{c}'(m)(\boldsymbol{c}(n) \otimes \boldsymbol{I}_{2M})\boldsymbol{Q}^{-1}\underline{\boldsymbol{B}}\boldsymbol{\varepsilon}(t) \\ &= \phi_{n+1,m}\eta_{n,m}(t) + \sum_{q=1}^{2N^2M} w_q^{(n,\imath)}\varepsilon_q(t) \end{aligned} \tag{39}$$

where $[w_1^{(n,m)} \;\ldots,\; w_{2N^2M}^{(n,m)}] = \boldsymbol{c}'(m)(\boldsymbol{c}(n) \otimes \boldsymbol{I}_{2M})\boldsymbol{Q}^{-1}\underline{\boldsymbol{B}}$.

Here, we can find that each $\eta_{n,m}(t)$ with $m \in \{1, \ldots, 2M\}$ is an Ornstein–Uhlenbeck process [42], [43]. It follows from [43, eq. (5.1.2)] that $\eta_{n,m}(t)$ satisfies the stochastic integral equation:

$$\eta_{n,m}(t) = \eta_{n,m}(0)e^{\phi_{n+1,m}t} + \sigma \sum_{q=1}^{2N^2M} w_q^{(n,\imath)} \int_0^t e^{\phi_{n+1,m}(t-s)} d\mathcal{B}_q(s)$$

where $\phi_{n+1,m} \leq 0$ and $\mathcal{B}_q(t)$ is defined in (27).

As shown in Appendix A, there exists a link between the Ornstein–Uhlenbeck process and autoregressive time series. We can apply this link to obtain (28), where

$$\widetilde{\varepsilon}_{n,m,k} := \sum_{q=1}^{N^2M} w_q^{(n,m)}\varepsilon_{n,m,q,k} \tag{40}$$

by letting $\varepsilon_{n,m,q,k} = \sigma \int_0^\tau e^{\phi_{n+1,m}(\tau-s')} d\mathcal{B}_q((k-1)\tau + s')$. It is easy to check that $\varepsilon_{n,m,q,k}$ is Gaussian with zero mean and variance $-(\sigma^2/2\phi_{n+1,m})(1 - e^{2\phi_{n+1,m}\tau})$, noting that the variance will be $\sigma^2\tau$ if $\phi_{n+1,m} = 0$. This means that $\widetilde{\varepsilon}_{n,m,k}$ is also Gaussian with zero mean, and the sequence $\{\widetilde{\varepsilon}_{n,m,k}\}_{k=1}^K$ has independent elements.

Hence, for any $n \in \{1, \ldots, N-1\}$ and any $m \in \{1, \ldots, 2M\}$, $\{\eta_{n,m,k}\}_{k=0}^K$ is a first-order autoregressive time series. By definition, $\{\eta_{n,m,k}\}_{k=0}^K$ is unit-root autoregressive if $\phi_{n+1,m} = 0$ (i.e., $e^{\phi_{n+1,m}\tau} = 1$). This completes the proof. ∎

Proof of Lemma 5: By using the definitions of $\boldsymbol{d}_{\imath,\ell}[k]$, $\underline{\boldsymbol{\xi}}_l(t)$, $\boldsymbol{\eta}_n(t)$, $\boldsymbol{\zeta}_n(t)$, and $\boldsymbol{\eta}_n[k]$, together with the relation

$$\boldsymbol{x}_\imath(k\tau) - \boldsymbol{x}_\ell(k\tau) = \sum_{n=1}^{N-1}\left(u_{\imath,n+1} - u_{\ell,n+1}\right)\underline{\boldsymbol{\xi}}_{n+1}(k\tau)$$

we can obtain (29) and thus prove the result. ∎

Proof of Lemma 6: First, (30) and (33) can be derived by using the following properties of the Euclidean inner product, trace, and vectorization: $\langle \boldsymbol{x}, \boldsymbol{y}\rangle = \boldsymbol{x}^T\boldsymbol{y} = \text{tr}(\boldsymbol{x}^T\boldsymbol{y})$ for vectors $\boldsymbol{x} \in \mathbb{R}^m$ and $\boldsymbol{y} \in \mathbb{R}^m$; $\text{tr}(\boldsymbol{XY}) = \text{tr}(\boldsymbol{YX})$ and $\text{tr}(\boldsymbol{X}^T\boldsymbol{Y}) = \text{vec}(\boldsymbol{X})^T\text{vec}(\boldsymbol{Y})$ for matrices $\boldsymbol{X} \in \mathbb{R}^{k\times l}$ and $\boldsymbol{Y} \in \mathbb{R}^{l\times m}$.

The next step of the proof is to show (31). We see that the term $\frac{\sum_{k=1}^K \boldsymbol{\eta}_{n_2}[k](\boldsymbol{\eta}_{n_1}[k-1])^T}{K^2}$ in (30) is a matrix whose (i,j)th entry is $\frac{\sum_{k=1}^K \eta_{n_2,i,k}\eta_{n_1,j,k-1}}{K^2}$, that is

$$\left[\frac{\sum_{k=1}^K \boldsymbol{\eta}_{n_2}[k]\left(\boldsymbol{\eta}_{n_1}[k-1]\right)^T}{K^2}\right]_{i,j} = \frac{\sum_{k=1}^K \eta_{n_2,i,k}\eta_{n_1,j,k-1}}{K^2} \tag{41}$$

where $i,j \in \{1, \ldots, 2M\}$. Using (28), we can show that

$$\begin{aligned} \frac{\sum_{k=1}^K \eta_{n_2,i,k}\eta_{n_1,j,k-1}}{K^2} &= \frac{\sum_{k=1}^K\left(e^{\phi_{n_2+1,i}\tau}\eta_{n_2,i,k-1} + \widetilde{\varepsilon}_{n_2,i,k}\right)\eta_{n_1,j,k-1}}{K^2} \\ &\xrightarrow{p} e^{\phi_{n_2+1,i}\tau}\frac{\sum_{k=1}^K \eta_{n_2,i,k-1}\eta_{n_1,j,k-1}}{K^2} \end{aligned} \tag{42}$$

where the convergence holds true since $\widetilde{\varepsilon}_{n_2,i,k}$ and $\eta_{n_1,j,k-1}$ are independent. Implicit in (42) is that the (i,j)th entry of $([\sum_{k=1}^K \boldsymbol{\eta}_{n_2}[k](\boldsymbol{\eta}_{n_1}[k-1])^T]/K^2)$ converges in probability to the (i,j)th entry of $e^{\boldsymbol{\Phi}_{n_2+1}\tau}([\sum_{k=1}^K \boldsymbol{\eta}_{n_2}[k-1](\boldsymbol{\eta}_{n_1}[k-1])^T]/K^2)$, where $e^{\boldsymbol{\Phi}_{n_2+1}\tau} = \sum_{q=1}^\infty(\tau^q/q!)\boldsymbol{\Phi}_{n_2+1}^q$ is a diagonal matrix since $\boldsymbol{\Phi}_{n_2+1}$ is diagonal. At this point, applying (41) and (42) to (30) results in (31).

Finally, using a fact about two matrices $\boldsymbol{X} \in \mathbb{R}^{k\times l}$ and $\boldsymbol{Y} \in \mathbb{R}^{l\times m}$ that $\text{vec}(\boldsymbol{XY}) = (\boldsymbol{I}_m \otimes \boldsymbol{X})\text{vec}(\boldsymbol{Y})$, for (31), we have

$$\begin{aligned} &\text{vec}\left(\frac{e^{\boldsymbol{\Phi}_{n_2+1}\tau}\sum_{k=1}^K \boldsymbol{\eta}_{n_2}[k-1]\left(\boldsymbol{\eta}_{n_1}[k-1]\right)^T}{K}\right) \\ &= \left(\boldsymbol{I}_{2M} \otimes e^{\boldsymbol{\Phi}_{n_2+1}\tau}\right)\text{vec}\left(\frac{\sum_{k=1}^K \boldsymbol{\eta}_{n_2}[k-1]\left(\boldsymbol{\eta}_{n_1}[k-1]\right)^T}{K}\right). \end{aligned}$$

Hence, (32) and (33) hold, which completes the proof. ■

Proof of Theorem 1: It is important to recall at this point that if agents $\imath$ and ℓ are disconnected, then it follows from Lemma 3 that $\phi_{2,1} = \cdots = \phi_{2,M} = 0$ (since $\lambda_2 = 0$ in this case), but $\phi_{2,M+1} = \cdots = \phi_{2,2M} < 0$ and $\phi_{i,1} = \cdots = \phi_{i,2M} < 0$ for all $i = 3, \ldots, N$.

Now, we evaluate $\frac{\sum_{k=1}^{K}\langle \boldsymbol{d}_{\imath,\ell}[k], \boldsymbol{d}_{\imath,\ell}[k-1]\rangle}{K^2}$ based on the expression in (31). On the one hand, if $n_1 = n_2 = 1$, then

$$\mathrm{vec}\left(\boldsymbol{\Theta}_2^T\boldsymbol{\Theta}_2\right)^T \mathrm{vec}\left(\frac{e^{\boldsymbol{\Phi}_2\tau}\sum_{k=1}^{K}\boldsymbol{\eta}_1[k-1]\left(\boldsymbol{\eta}_1[k-1]\right)^T}{K^2}\right)$$
$$= \mathrm{vec}(\boldsymbol{I}_{2M})^T \mathrm{vec}\left(\frac{e^{\boldsymbol{\Phi}_2\tau}\sum_{k=1}^{K}\boldsymbol{\eta}_1[k]\left(\boldsymbol{\eta}_1[k-1]\right)^T}{K^2}\right)$$
$$= \sum_{i=1}^{2M} e^{\phi_{2,i}\tau}\frac{\sum_{k=1}^{K}\eta_{1,i,k-1}^2}{K^2} \xrightarrow{p} \sum_{i=1}^{M}\frac{\sum_{k=1}^{K}\eta_{1,i,k-1}^2}{K^2}. \quad (43)$$

The convergence in (43) follows from (42) and Proposition 4. That is, for each $i \in \{M+1, \ldots, 2M\}$, $\{\eta_{1,i,k-1}\}_{k=0}^{K}$ is not unit-root autoregressive since $e^{\phi_{2,i}\tau} < 1$, such that $([\sum_{k=1}^{K}\eta_{1,i,k-1}^2]/K^2) \xrightarrow{p} 0$; however, for each $i \in \{1, \ldots, M\}$, $\{\eta_{1,i,k-1}\}_{k=0}^{K}$ is unit-root autoregressive because $e^{\phi_{2,i}\tau} = 1$. It follows from Lemma 4 and Proposition 4 that:

$$\frac{\sum_{k=1}^{K}\eta_{1,i,k-1}^2}{K^2} \xrightarrow{L} \sigma_{m,n}^2\int_0^1[\mathcal{B}'(s)]^2 ds, \quad i \in \{1, \ldots, M\} \quad (44)$$

where $\sigma_{m,n}^2 = \sigma^2\tau\|\boldsymbol{c}'(m)(\boldsymbol{c}(n)\otimes\boldsymbol{I}_{2M})\boldsymbol{Q}^{-1}\underline{\boldsymbol{B}}\|_2^2$.

On the other hand, if $n_1 \neq 1$ or $n_2 \neq 1$, it is easy to see that

$$\left|\frac{\sum_{k=1}^{K}\eta_{n_2,i,k-1}\eta_{n_1,j,k-1}}{K^2}\right| \leq \sqrt{\frac{\sum_{k=1}^{K}\eta_{n_2,i,k-1}^2}{K^2}}\sqrt{\frac{\sum_{k=1}^{K}\eta_{n_1,j,k-1}^2}{K^2}} \quad (45)$$

by Hölder's inequality [44]. Without loss of generality, we assume that $n_1 \neq 1$, and obtain $\sqrt{([\sum_{k=1}^{K}\eta_{n_1,j,k-1}^2]/K^2)} \xrightarrow{p} 0$ such that $([\sum_{k=1}^{K}\eta_{n_2,i,k-1}\eta_{n_1,j,k-1}]/K^2) \xrightarrow{p} 0$. This further allows us to have

$$\frac{e^{\phi_{2,i}\tau}\sum_{k=1}^{K}\eta_{n_2,i,k-1}\eta_{n_1,j,k-1}}{K^2} \xrightarrow{p} 0. \quad (46)$$

Substituting (43)–(46) into (31) and letting $\widetilde{\eta}_{1,i} = ([\sum_{k=1}^{K}\eta_{1,i,k-1}^2]/K^2)$ yields

$$\frac{\sum_{k=1}^{K}\langle \boldsymbol{d}_{\imath,\ell}[k], \boldsymbol{d}_{\imath,\ell}[k-1]\rangle}{K^2} \xrightarrow{p} \widetilde{u}_{1,1}\sum_{i=1}^{M}\widetilde{\eta}_{1,i} \quad (47)$$

where $\widetilde{\eta}_{1,i} \xrightarrow{L} \sigma_{m,n}^2\int_0^1[\mathcal{B}'(s)]^2 ds$, $i \in \{1, \ldots, M\}$, that is, (35) is derived.

Similar to the derivations of (35), we can also evaluate $([\sum_{k=1}^{K}\langle \boldsymbol{d}_{\imath,\ell}[k-1], \boldsymbol{d}_{\imath,\ell}[k-1]\rangle]/K^2)$ and obtain (36).

After obtaining (35) and (36), we finally complete the proof by applying [40, Example 7.2] to show that $\rho_{\imath,\ell}^K \xrightarrow{p} 1$. ■

Proof of Theorem 2: This is an immediate consequence of Theorem 1. Specifically, under the same assumption as Theorem 1, we first obtain $\rho_{\imath,\ell}^K \xrightarrow{p} 1$ and then use the definition of convergence in probability to show that for all $C \in (0, 1)$, the miss probability satisfies $\lim_{K\to\infty} P(|\rho_{\imath,\ell}^K - 1| \geq C|\text{Disconnected}) = 0$. ■

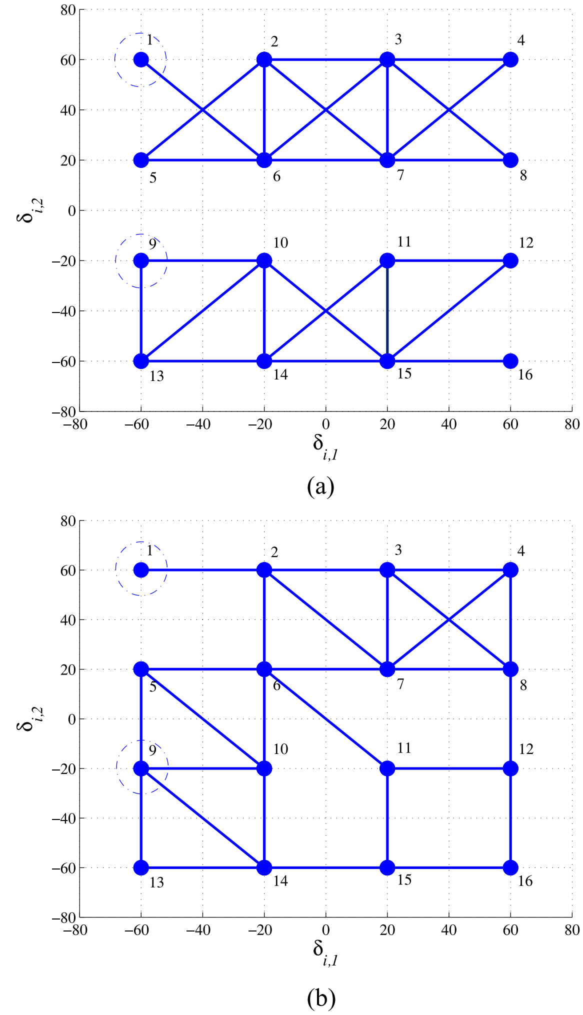

Fig. 4. Two cases considered in the simulations, which have the same desired formation shape but different communication graphs $\mathcal{G}_a$. Note that the formation shape is specified by parameters $\boldsymbol{\delta}_i$. (a) Disconnected case (i.e., agents $\imath = 1$ and $\ell = 9$ are disconnected), which implies that the hypothesis H_1 as in (17) is true. (b) Connected case (i.e., agents $\imath = 1$ and $\ell = 9$ are connected), which implies that the hypothesis H_0 as in (16) is true.

V. Simulations

In this section, we present simulation results of the proposed Decision Rule 2 and Procedure 1 available to external estimators for a multiagent system (8) with 16 agents. The simulations are performed in $\mathbb{R}^2$ space with initial conditions $\boldsymbol{p}_i(0) = \boldsymbol{\delta}_i + \boldsymbol{w}_i$ and $\boldsymbol{v}_i(0) = \boldsymbol{0}_2$ for all $i \in \{1, \ldots, 16\}$, where $\boldsymbol{w}_i = [w_{i,1}\ w_{i,2}]^T \in \mathbb{R}^2$ whose entries satisfy $w_{i,m} \sim \mathcal{N}(0, 40^2)$. As such, we can write $\boldsymbol{\delta}_i = [\delta_{i,1}\ \delta_{i,2}]^T$ and $\boldsymbol{p}_i(t) = [p_{i,1}(t)\ p_{i,2}(t)]^T$. For the control law (9), we let $\alpha = 1.0$ and $\beta = 2.9$. Without loss of generality, the disconnectedness between agents $\imath = 1$ and $\ell = 9$ are of interest, and we set $\tau = 3$.

To provide comparative performance plots, let us consider two cases as illustrated in Fig. 4. More specifically, one is the disconnected case, that is, the case in which agents $\imath = 1$ and

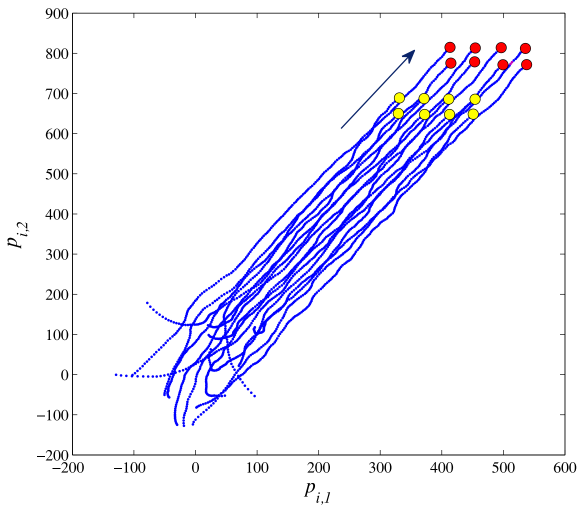

(a)

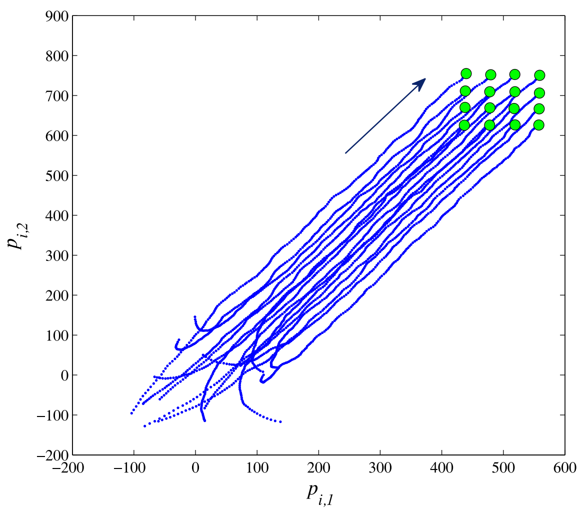

(b)

Fig. 5. Position trajectories and achieved formation shapes in the disconnected and connected cases. (a) Disconnected case (one trial). (b) Connected case (one trial).

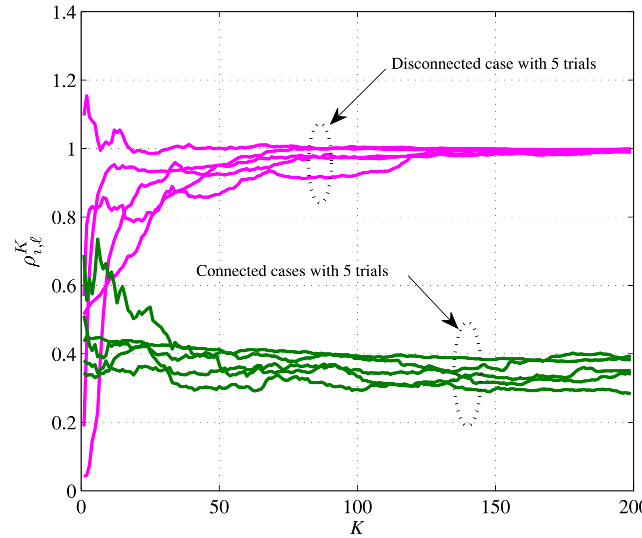

Fig. 6. Evolution of $\rho^K_{\imath,\ell}$ as K increases in both disconnected and connected cases.

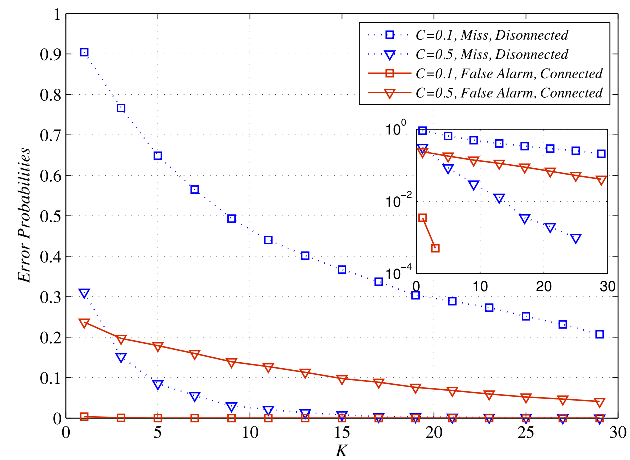

Fig. 7. Error probabilities of Decision Rule 2 as K increases, that is, miss and false alarm probabilities for disconnected and connected cases, respectively. Different values of C are used, including $C = 0.1$ and $C = 0.5$. The inset plots the data of error probabilities as logarithmic scale for the y-axis.

$\ell = 9$ are disconnected, and the other is the connected case, that is, the case in which two agents are connected. These two cases are related to H_1 and H_0 hypotheses specified by (17) and (16), respectively. In Fig. 5(a) and (b), we show position trajectories and achieved formation shapes in the disconnected and connected cases with one trial, respectively. It can be seen from Fig. 5(a) that the desired formation shape cannot be achieved in the disconnected case since the communication graph is disconnected.

Numerical examples of $\rho^K_{\imath,\ell}$ are provided in Fig. 6, where we show the behavior of $\rho^K_{\imath,\ell}$ as K increases in both disconnected and connected cases with five trials. The results show us an obvious contrast between the disconnected and connected cases with respect to the behavior of $\rho^K_{\imath,\ell}$. That is, in the disconnected case, $\rho^K_{\imath,\ell}$ approaches 1 as K increases, while in the connected case, it appears that $\rho^K_{\imath,\ell}$ is evidently less than 1. In addition, Fig. 6 shows that $\rho^K_{\imath,\ell}$ has already become close to 1 when $K \leq 200$ in the disconnected case.

The error probabilities of Decision Rule 2 in both disconnected and connected cases are plotted in Fig. 7. Simulation results of the miss and false alarm probabilities are provided for $C = 0.1$ and $C = 0.5$. As expected by Theorem 1, the miss probability $P(|\rho^K_{\imath,\ell} - 1| > C|\text{Disconnected})$ decays with growing K in the disconnected case. Also it can be seen that the false alarm probability $P(|\rho^K_{\imath,\ell} - 1| \leq C|\text{Connected})$ quickly decreases as K grows larger in the connected case. Perhaps the most inspiring finding is that with $C = 0.5$ both the miss and false alarm probabilities can be reduced to less than 0.05 with $K = 30$. By comparing the performances with $C = 0.1$ and with $C = 0.5$, we see that there is no significant difference in the rates of decrease of miss and false alarm probabilities with $C = 0.5$, while the miss probability decreases much more slowly than the false alarm probability with $C = 0.1$. Thus, as mentioned in Section III, we propose to set $C = 0.5$, because

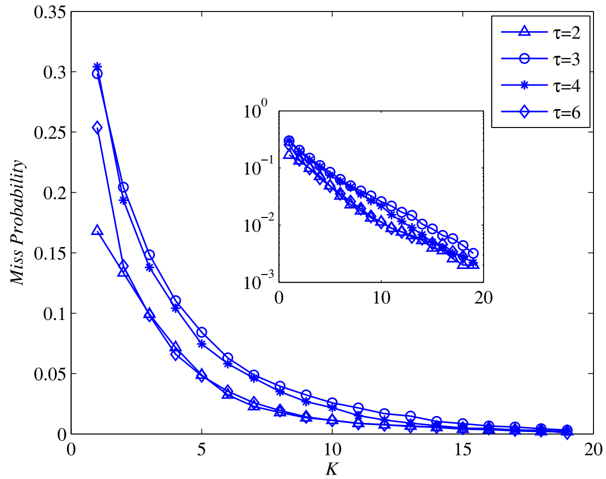

Fig. 8. Miss probability of Decision Rule 2 as K increases, for different τ in the disconnected case. The inset plots the data of miss probability as logarithmic scale for the y-axis.

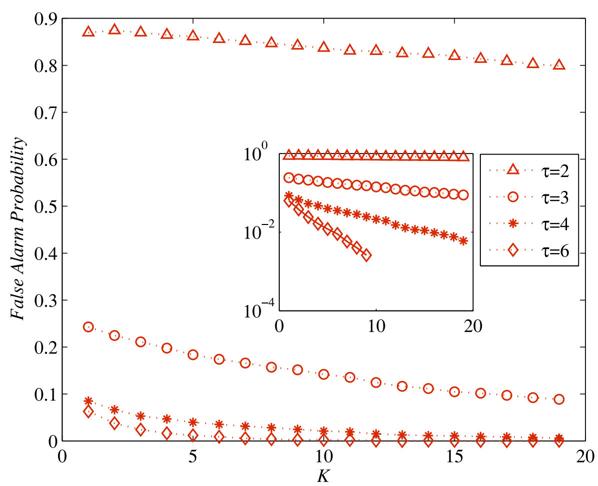

Fig. 9. False alarm probability of Decision Rule 2 as K increases, for different τ in the connected case. The inset plots the data of false alarm probability as logarithmic scale for the y-axis.

it turns out numerically that $C = 0.5$ (i.e., the median of 0 and 1) is an appropriate threshold for Decision Rule 2 and makes it simple to apply the decision rule in practice.

In Fig. 8, the miss probability of Decision Rule 2 is depicted for different values of τ in the disconnected case. We see that the miss probability can quickly decay to 0 in the disconnected case with $\tau = 2, 3, 4, 6$. It seems from the inset of Fig. 8 that the value of τ does not have an apparent effect on the decaying rate of the miss probability. This observation is consistent with Theorems 1 and 2 that do not make an additional assumption about τ. In other words, Theorems 1 and 2 always hold true regardless of the value of τ, meaning that the miss probability can always converge to 0 in the disconnected case.

For comparison, the false alarm probability of Decision Rule 2 with different values of τ in the connected case is illustrated by Fig. 9. It is shown that the false alarm probability behaves differently as τ varies. We can see that in the connected case with $\tau = 3, 4, 6$, the false alarm probability can decrease to be less than 0.05 when K reaches 20; however, with $\tau = 2$, the

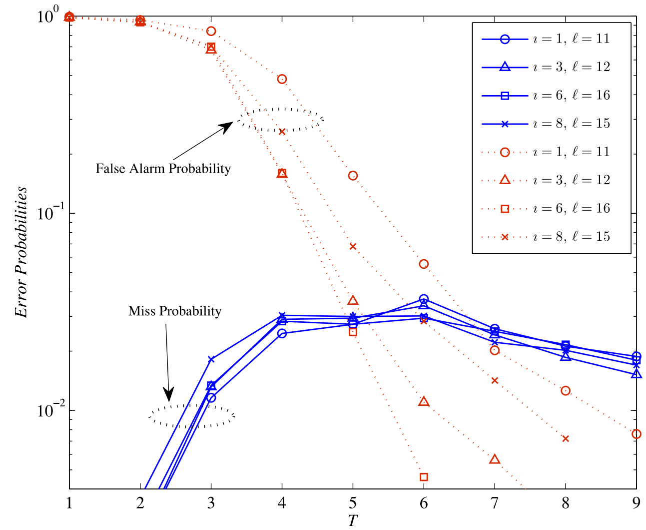

Fig. 10. Error probabilities of the decision made in Procedure 1 with $\tau = f(\tau_0, T) = \tau_0 T$, for different agent pairs in both disconnected and connected cases.

false alarm probability is relatively large and cannot decrease to the small value for $K \leq 20$. These results tell us that the value of τ can affect the false alarm probability, that is, the larger τ is, the smaller the false alarm probability is likely to be. This can be explained by Remark 4.

To illustrate the effectiveness of Procedure 1, we perform simulations by setting $\tau_0 = 1$, $K = 10$, and considering four agent pairs, that is, $(\imath = 1, \ell = 11)$, $(\imath = 3, \ell = 12)$, $(\imath = 6, \ell = 16)$, and $(\imath = 8, \ell = 15)$. Fig. 10 plots the error probabilities of the decision made in Procedure 1, from which two important trends can be observed. First, the miss probability can always be small and does not significantly decrease as τ increases ($\tau = \tau_0 T$), as we have already observed from Fig. 8. Second, the false alarm probability will become considerably small as τ grows, even if this probability is initially large (close to 1). This implies that using large τ in Procedure 1 (if allowed) can effectively improve the false alarm performance of the decision, as we can expect from Remark 4.

VI. Conclusion

This article provides an approach to monitoring the connection status of two arbitrarily chosen agents via external estimators and to identifying those that are disconnected, based on the sampled data. We design a decision rule to realize this kind of identification for formation-control multiagent systems and prove that the miss probability of this rule converges to 0 as the number of data samples increases. Interestingly, both miss and false alarm probabilities can be reduced to below 0.05 in many simulated cases with only a small sample number. The ability to identify disconnected agents in multiagent systems is important for practical purposes, as it allows actions to be taken to reconnect the disconnected agents. This study is only a first step in this direction, and considerable effort is needed to improve the decision rule, develop more powerful analysis methods, and devise reconnection strategies. Extending the derived results to multiagent systems using the control laws with random errors other than white noise is also meaningful for future work.

Appendix A
Link Between Ornstein–Uhlenbeck Process and Autoregressive Time Series

Definition [42], [43]: The Ornstein–Uhlenbeck process is the solution $X(t)$ of the stochastic differential equation $dX(t) = -\alpha X(t)dt + \sigma d\mathcal{B}(t)$ with $X(0) = x_0$, where $\alpha \geq 0$ and $\sigma > 0$ are constants. This solution can be expressed by $X(t) = x_0 e^{-\alpha t} + \sigma \int_0^t e^{-\alpha(t-s)} d\mathcal{B}(s)$.

Lemma A1: Let X_k be the samples of the Ornstein–Uhlenbeck process $X(t)$ taken at $t = k\tau$, where $k = 0, 1, \ldots,$ and τ is the sampling interval. Then, X_k is an autoregressive time series, satisfying $X_k = e^{-\alpha\tau} X_{k-1} + \varepsilon'_k$, where $\varepsilon'_k = \sigma \int_0^\tau e^{-\alpha(\tau-s')} d\mathcal{B}((k-1)\tau + s') \sim \mathcal{N}(0, (\sigma^2/2\alpha)(1 - e^{-2\alpha\tau}))$ and the $\{\varepsilon'_k\}$ sequence has independent elements, that is, ε'_{k_1} and ε'_{k_2} are independent for $k_1 \neq k_2$.

Proof: Since $X_k = x_0 e^{-\alpha k\tau} + \sigma \int_0^{k\tau} e^{-\alpha(k\tau-s)} d\mathcal{B}(s)$, we can have $X_k = e^{-\alpha\tau} X_{k-1} + \sigma \int_{(k-1)\tau}^{k\tau} e^{-\alpha(k\tau-s)} d\mathcal{B}(s) = e^{-\alpha\tau} X_{k-1} + \sigma \int_0^\tau e^{-\alpha(\tau-s')} d\mathcal{B}((k-1)\tau + s') = e^{-\alpha\tau} X_{k-1} + \varepsilon'_k$. To derive the properties of ε'_k, we need to use some basic facts of Brownian motion. First, $\mathcal{B}(s')$ is time homogeneous that means $\mathcal{B}(s')$ and $\mathcal{B}((k-1)\tau + s')$ have the same distribution [43, eq. (7.1.6)]. Second, a $d\mathcal{B}(s')$ integral of a deterministic process will yield a Gaussian process [42, Proposition 7.6], so ε'_k is Gaussian with mean 0 and variance $(\sigma^2/2\alpha)(1 - e^{-2\alpha\tau})$ according to the Itô isometry [43, Corollary 3.1.7]. Third, the independence of the elements in $\{\varepsilon'_k\}_{k=1}^\infty$ holds true because $\mathcal{B}(s')$ has independent increments. ■

References

[1] Y. Zhang, S. Li, and J. Weng, "Distributed estimation of algebraic connectivity," *IEEE Trans. Cybern.*, vol. 52, no. 5, pp. 3047–3056, May 2022.

[2] J. Fu, G. Wen, X. Yu, and Z.-G. Wu, "Distributed formation navigation of constrained second-order multiagent systems with collision avoidance and connectivity maintenance," *IEEE Trans. Cybern.*, vol. 52, no. 4, pp. 2149–2162, Apr. 2022.

[3] P. D. Hung, T. Q. Vinh, and T. D. Ngo, "Hierarchical distributed control for global network integrity preservation in multirobot systems," *IEEE Trans. Cybern.*, vol. 50, no. 3, pp. 1278–1291, Mar. 2020.

[4] Z. Kan, E. A. Doucette, and W. E. Dixon, "Distributed connectivity preserving target tracking with random sensing," *IEEE Trans. Autom. Control*, vol. 64, no. 5, pp. 2166–2173, May 2019.

[5] B. Ning, Q.-L. Han, Z. Zuo, J. Jin, and J. Zheng, "Collective behaviors of mobile robots beyond the nearest neighbor rules with switching topology," *IEEE Trans. Cybern.*, vol. 48, no. 5, pp. 1577–1590, May 2018.

[6] R. Dutta, L. Sun, and D. Pack, "A decentralized formation and network connectivity tracking controller for multiple unmanned systems," *IEEE Trans. Control Syst. Technol.*, vol. 26, no. 6, pp. 2206–2213, Nov. 2018.

[7] H. Fang, Y. Wei, J. Chen, and B. Xin, "Flocking of second-order multiagent systems with connectivity preservation based on algebraic connectivity estimation," *IEEE Trans. Cybern.*, vol. 47, no. 4, pp. 1067–1077, Apr. 2017.

[8] D. Boskos and D. Dimarogonas, "Robustness and invariance of connectivity maintenance control for multiagent systems," *SIAM J. Control Optim.*, vol. 55, no. 3, pp. 1887–1914, 2017.

[9] A. Gasparri, L. Sabattini, and G. Ulivi, "Bounded control law for global connectivity maintenance in cooperative multirobot systems," *IEEE Trans. Robot.*, vol. 33, no. 3, pp. 700–717, Jun. 2017.

[10] L. Sabattini, C. Secchi, and N. Chopra, "Decentralized estimation and control for preserving the strong connectivity of directed graphs," *IEEE Trans. Cybern.*, vol. 45, no. 10, pp. 2273–2286, Oct. 2015.

[11] M. Fiacchini and I.-C. Morărescu, "Convex conditions on decentralized control for graph topology preservation," *IEEE Trans. Autom. Control*, vol. 59, no. 6, pp. 1640–1645, Jun. 2014.

[12] R. Aragues, D. Shi, D. V. Dimarogonas, C. Sagüés, K. H. Johansson, and Y. Mezouar, "Distributed algebraic connectivity estimation for undirected graphs with upper and lower bounds," *Automatica*, vol. 50, no. 12, pp. 3253–3259, Dec. 2014.

[13] P. Di Lorenzo and S. Barbarossa, "Distributed estimation and control of algebraic connectivity over random graphs," *IEEE Trans. Signal Process.*, vol. 62, no. 21, pp. 5615–5628, Nov. 2014.

[14] M. Franceschelli, A. Gasparri, A. Giua, and C. Seatzu, "Decentralized estimation of Laplacian Eigenvalues in multi-agent systems," *Automatica*, vol. 49, no. 4, pp. 1031–1036, Apr. 2013.

[15] M. M. Zavlanos and G. J. Pappas, "Distributed connectivity control of mobile networks," *IEEE Trans. Robot.*, vol. 24, no. 6, pp. 1416–1428, Dec. 2008.

[16] L. Sabattini, N. Chopra, and C. Secchi, "Decentralized connectivity maintenance for cooperative control of mobile robotic systems," *Int. J. Robot. Res.*, vol. 32, no. 12, pp. 1411–1423, Oct. 2013.

[17] Z. Kan, A. P. Dani, J. M. Shea, and W. E. Dixon, "Network connectivity preserving formation stabilization and obstacle avoidance via a decentralized controller," *IEEE Trans. Autom. Control*, vol. 57, no. 7, pp. 1827–1832, Jul. 2012.

[18] M. M. Zavlanos, M. B. Egerstedt, and G. J. Pappas, "Graph-theoretic connectivity control of mobile robot networks," *Proc. IEEE*, vol. 99, no. 9, pp. 1525–1540, Sep. 2011.

[19] A. Ajorlou, A. Momeni, and A. G. Aghdam, "A class of bounded distributed control strategies for connectivity preservation in multi-agent systems," *IEEE Trans. Autom. Control*, vol. 55, no. 12, pp. 2828–2833, Dec. 2010.

[20] P. Yang, R. A. Freeman, G. J. Gordon, K. M. Lynch, S. S. Sriniasa, and R. Sukthankar, "Decentralized estimation and control of graph connectivity for mobile sensor networks," *Automatica*, vol. 46, no. 2, pp. 390–396, 2010.

[21] D. V. Dimarogonas and K. J. Kyriakopoulos, "Connectedness preserving distributed swarm aggregation for multiple kinematic robots," *IEEE Trans. Robot.*, vol. 24, no. 5, pp. 1213–1223, Oct. 2008.

[22] M. Ji and M. Egerstedt, "Distributed coordination control of multiagent systems while preserving connectedness," *IEEE Trans. Robot.*, vol. 23, no. 4, pp. 693–703, Aug. 2007.

[23] M. C. De Gennaro and A. Jadbabaie, "Decentralized control of connectivity for multi-agent systems," in *Proc. IEEE Conf. Decis. Control (CDC)*, San Diego, CA, USA, Dec. 2006, pp. 3628–3633.

[24] Y. Kantaros and M. M. Zavlanos, "Distributed intermittent connectivity control of mobile robot networks," *IEEE Trans. Autom. Control*, vol. 62, no. 7, pp. 3109–3121, Jul. 2017.

[25] R. Khodayi-Mehr, Y. Kantaros, and M. M. Zavlanos, "Distributed state estimation using intermittently connected robot networks," *IEEE Trans. Robot.*, vol. 35, no. 3, pp. 709–724, Jun. 2019.

[26] R. Aragues, D. V. Dimarogonas, P. Guallar, and C. Sagues, "Intermittent connectivity maintenance with heterogeneous robots," *IEEE Trans. Robot.*, vol. 37, no. 1, pp. 225–245, Feb. 2021.

[27] K. You and L. Xie, "Network topology and communication data rate for consensusability of discrete-time multi-agent systems," *IEEE Trans. Autom. Control*, vol. 56, no. 10, pp. 2262–2275, Oct. 2011.

[28] H. Wang, H. Zhao, J. Zhang, D. Ma, J. Li, and J. Wei, "Survey on unmanned aerial vehicle networks: A cyber physical system perspective," *IEEE Commun. Surveys Tuts.*, vol. 22, no. 2, pp. 1027–1070, 2nd Quart., 2020.

[29] L. Gupta, R. Jain, and G. Vaszkun, "Survey of important issues in UAV communication networks," *IEEE Commun. Surveys Tuts.*, vol. 18, no. 2, pp. 1123–1152, 2nd Quart., 2016.

[30] A. B. Farjadian, B. Thomsen, A. M. Annaswamy, and D. D. Woods, "Resilient flight control: An architecture for human supervision of automation," *IEEE Trans. Control Syst. Technol.*, vol. 29, no. 1, pp. 29–42, Jan. 2021.

[31] Z. Li and J. Chen, "Robust consensus of linear feedback protocols over uncertain network graphs," *IEEE Trans. Autom. Control*, vol. 62, no. 8, pp. 4251–4258, Aug. 2017.

[32] T. Li and J.-F. Zhang, "Consensus conditions of multi-agent systems with time-varying topologies and stochastic communication noises," *IEEE Trans. Autom. Control*, vol. 55, no. 9, pp. 2043–2057, Sep. 2010.

[33] W. Ren, "Consensus strategies for cooperative control of vehicle formations," *IET Control Theory Appl.*, vol. 1, no. 2, pp. 505–512, Mar. 2007.

[34] K.-K. Oh, M.-C. Park, and H.-S. Ahn, “A survey of multi-agent formation control,” *Automatica*, vol. 53, pp. 424–440, Mar. 2015.
[35] R. Qian, Z. Duan, Y. Qi, T. Peng, and W. Wang, “Formation-control stability and communication capacity of multiagent systems: A joint analysis,” *IEEE Trans. Control Netw. Syst.*, vol. 8, no. 2, pp. 917–927, Jun. 2021.
[36] B. Ning, Q.-L. Han, and Z. Zuo, “Distributed optimization for multiagent systems: An edge-based fixed-time consensus approach,” *IEEE Trans. Cybern.*, vol. 49, no. 1, pp. 122–132, Jan. 2019.
[37] U. Luxburg, “A tutorial on spectral clustering,” *Stat. Comput.*, vol. 17, no. 4, pp. 395–416, 2007.
[38] D. West, *Introduction to Graph Theory*, 2nd ed. Singapore: Pearson Educ., 2001.
[39] C. Godsil and G. Royle, *Algebraic Graph Theory*. New York, NY, USA: Springer, 2001.
[40] J. Hamilton, *Time Series Analysis*. Princeton, NJ, USA: Princeton Univ. Press, 1994.
[41] H. V. Poor, *An Introduction to Signal Detection and Estimation*, 2nd ed. New York, NY, USA: Springer-Verlag, 1994.
[42] J. Steele, *Stochastic Calculus and Financial Applications*. New York, NY, USA: Springer-Verlag, 2001.
[43] B. Øksendal, *Stochastic Differential Equations—An Introduction With Applications*. Berlin, Germany: Springer, 1998.
[44] I. Gradshteyn, I. Ryzhik, A. Jeffrey, and D. Zwillinger, *Table of Integrals, Series, and Products*, 7th ed. Boston, MA, USA: Academic, 2007.
[45] Z. Li and Z. Duan, *Cooperative Control of Multi-Agent Systems: A Consensus Region Approach*. Boca Raton, FL, USA: CRC Press, 2014.
[46] J. Blitzstein and J. Hwang, *Introduction to Probability*. Boca Raton, FL, USA: CRC Press, 2014.

Rongrong Qian (Member, IEEE) received the B.S. degree in communication engineering and the Ph.D. degree in signal and information processing from the Beijing University of Posts and Telecommunications (BUPT), Beijing, China, in 2004 and 2010, respectively.

From 2010 to 2020, he was a Lecturer and an Associate Professor with the School of Automation, BUPT, where he is currently an Associate Professor with the School of Artificial Intelligence. From July 2015 to June 2016, he was a Visiting Scholar with the College of Engineering, Peking University, Beijing. His research interests include multiagent systems, networked control systems, and wireless networks, with applications to UAV swarms and mobile robots.

Zhisheng Duan (Senior Member, IEEE) received the M.S. degree in mathematics from Inner Mongolia University, Hohhot, China, in 1997, and the Ph.D. degree in control theory from Peking University, Beijing, China, in 2000.

From 2000 to 2002, he worked as a Postdoctoral Fellow with Peking University. Since 2008, he has been a Professor with the Department of Mechanics and Aerospace Engineering, College of Engineering, Peking University, where he is currently a Changjiang Scholar. His research interests include robust control, stability of interconnected systems, and analysis and control of complex dynamical networks.

Prof. Duan received the 2001 Chinese Control Conference Guan-Zhao Zhi Award, the 2011 First Class Award in Natural Science from Chinese Ministry of Education, and the 2015 Second Class Award of National Natural Science. He obtained the Outstanding Youth Fund of National Natural Science in 2012.

Yuan Qi received the B.S. degree in communication engineering and the Ph.D. degree in signal and information processing from the Beijing University of Posts and Telecommunications (BUPT), Beijing, China, in 2004 and 2009, respectively.

From 2009 to 2020, she was a Lecturer with the School of Electronic Engineering, BUPT, where she is currently an Associate Professor. Her research interests include multiagent networks, millimeter-wave communications, and signal processing in wireless communications.

Tao Peng (Member, IEEE) received the bachelor’s, master’s, and Ph.D. degrees from the Beijing University of Posts and Telecommunications (BUPT), Beijing, China, in 1999, 2002, and 2010, respectively.

He is currently an Associate Professor with BUPT, where he has been the Chair of Device-to-Device (D2D) Technical Discussion Group of IMT-A/IMT-2020 Propulsion Group in CCSA. He has authored over 70 academic papers with 16 SCI indexed, and an inventor of 25 international and domestic patents. His research interests include cognitive radio and software-defined radio, D2D communication, CRAN and ultradense networks, and mobile ad hoc network.

Wenbo Wang (Senior Member, IEEE) received the B.S. degree in communication engineering and the M.S. and Ph.D. degrees in signal and information processing from the Beijing University of Posts and Telecommunications (BUPT), Beijing, China, in 1986, 1989, and 1992, respectively.

From October 1992 to 1993, he was a Researcher with ICON Communication Inc., Dallas, TX, USA. He has been a Chair Professor with the School of Information and Communications Engineering, BUPT, where he is currently the Vice President. He is also the Assistant Director of the Universal Wireless Communication Laboratory, BUPT. He has also been the Director of the Beijing Institute of Communication, Beijing, since 2002, and an Assistant Director of the National Defense Communication Committee, China Institute of Communication. He has published more than 200 articles and six books and holds 12 patents. His research interests include transmission technology, broadband wireless access, wireless network theory, digital signal processing, multiple-input–multiple-output, cooperative and cognitive communications, and software radio technology.